

Deep Learning Based 3D Segmentation: A Survey^{*}

Yong He^a, Hongshan Yu^{a,*}, Xiaoyan Liu^a, Zhengeng Yang^a, Wei Sun^a and Ajmal Mian^b

^aHunan University, Lushan South Rd., Yuelu Dist., Changsha, 410082, Hunan, China

^bUniversity of Western Australia, 35 Stirling Hwy, Perth, 6009, WA, Australia

ARTICLE INFO

Keywords:

3D data
3D semantic segmentation
3D instance segmentation
3D part segmentation
3D video segmentation
3D semantic map
Deep learning

ABSTRACT

3D segmentation is a fundamental and challenging problem in computer vision with applications in autonomous driving, robotics, augmented reality and medical image analysis. It has received significant attention from the computer vision, graphics and machine learning communities. Conventional methods for 3D segmentation, based on hand-crafted features and machine learning classifiers, lack generalization ability. Driven by their success in 2D computer vision, deep learning techniques have recently become the tool of choice for 3D segmentation tasks. This has led to an influx of a large number of methods in the literature that have been evaluated on different benchmark datasets. Whereas survey papers on RGB-D and point cloud segmentation exist, there is a lack of an in-depth and recent survey that covers all 3D data modalities and application domains. This paper fills the gap and provides a comprehensive survey of the recent progress made in deep learning based 3D segmentation. It covers over 180 works, analyzes their strengths and limitations and discusses their competitive results on benchmark datasets. The survey provides a summary of the most commonly used pipelines and finally highlights promising research directions for the future.

1. Introduction

Segmentation of 3D scenes is a fundamental and challenging problem in computer vision as well as computer graphics. The objective of 3D segmentation is to build computational techniques that predict the fine-grained labels of objects in a 3D scene for a wide range of applications such as autonomous driving, mobile robots, industrial control, augmented reality and medical image analysis. As illustrated in Figure 1, 3D segmentation can be divided into three types: semantic, instance and part segmentation. Semantic segmentation aims to predict object class labels such as table and chair. Instance segmentation additionally distinguishes between different instances of the same class labels e.g. table one/two and chair one/two. Part segmentation aims to decompose instances further into their different components such as armrests, legs and backrest of the same chair.

Compared to conventional single view 2D segmentation, 3D segmentation gives a more comprehensive understanding of a scene, since 3D data (e.g. RGB-D, point cloud, voxel, mesh, 3D video) contain richer geometric, shape, and scale information with less background noise. Moreover, the representation of 3D data, for example in the form of projected images, has more semantic information.

Recently, deep learning techniques have dominated many research areas including computer vision and natural language processing. Motivated by its success in learning powerful features, deep learning for 3D segmentation has

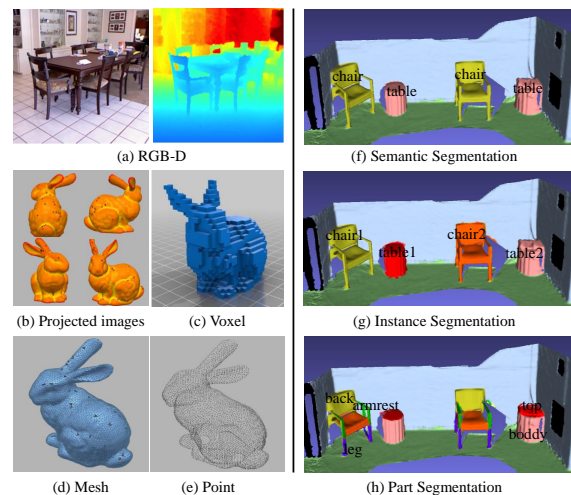


Fig. 1: The main five types of 3D data: (a) RGB-D image, (b) projected images, (c) voxels, (d) mesh, and (d) point. Types of 3D segmentation: (f) 3D semantic segmentation, (g) 3D instance segmentation, and (h) 3D part segmentation.

also attracted a growing interest from the research community over the past decade. However, 3D deep learning methods still face many unsolved challenges. For example, irregularity of point clouds makes it difficult to exploit local features and converting them to high-resolution voxels comes with a huge computational burden.

This paper provides a comprehensive survey of recent progress in deep learning methods for 3D segmentation. It focuses on analyzing commonly used building blocks, convolution kernels and complete architectures pointing out the pros and cons in each case. The survey covers over 180 representative papers published in the last five years. Although some notable 3D segmentation surveys have been released including RGB-D semantic segmentation [Fooladgar](#)

^{*}This work was partially supported by the National Natural Science Foundation of China (Grant U2013203, 61973106). Professor Ajmal Mian is the recipient of an Australian Research Council Future Fellowship Award (project number FT210100268) funded by the Australian Government.

*Corresponding author

✉ h.yong@hnu.edu.cn (Y. He); yuhongshancn@hotmail.com (H. Yu);
xiaoyan.liu@hnu.edu.cn (X. Liu); yzg050215@163.com (Z. Yang);
david-sun@126.com (W. Sun); ajmal.mian@uwa.edu.au (A. Mian)

ORCID(s): 0000-0003-2916-3068 (Y. He); 0000-0003-1973-6766 (H. Yu)

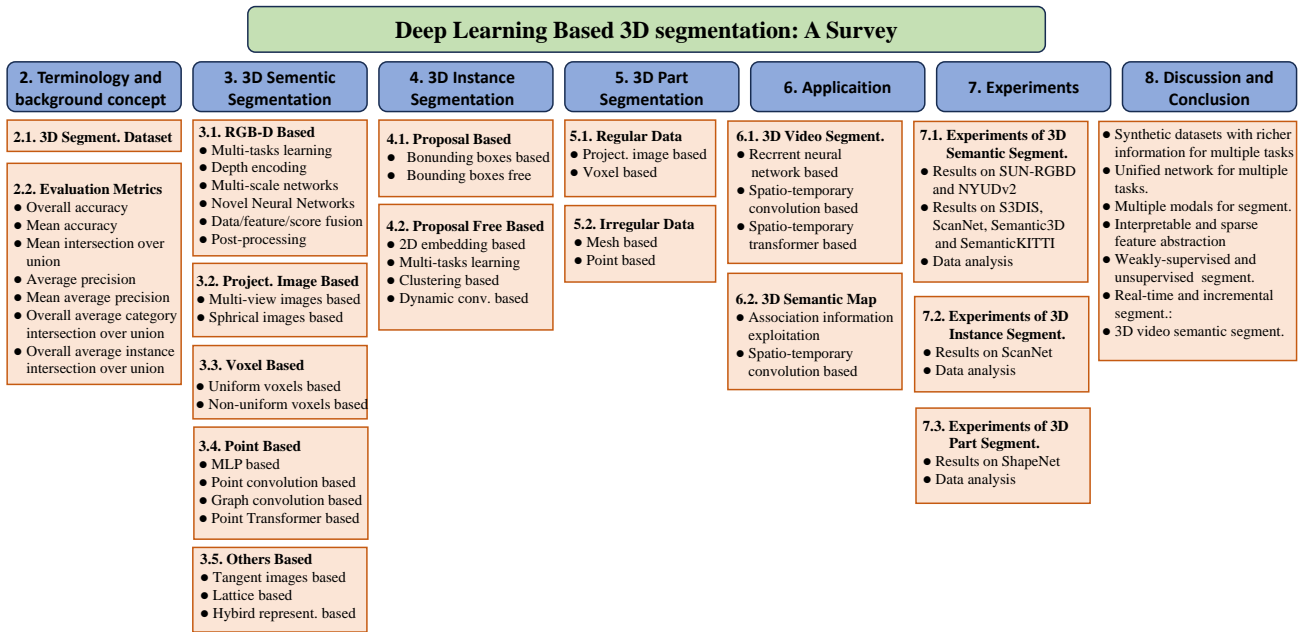


Fig. 2: Complete overview of the survey paper.

and Kasaei (2020), remote sensing imagery segmentation Yuan, Shi and Gu (2021), point clouds segmentation Xie, Jiaojiao and Zhu (2020a), Guo, Wang, Hu, Liu, Liu and Benmamoun (2020), Liu, Sun, Li, Hu and Wang (2019a), Bello, Yu, Wang, Adam and Li (2020), Naseer, Khan and Porikli (2018), Ioannidou, Chatzilari, Nikolopoulos and Kompatsiaris (2017), these surveys do not comprehensively cover all 3D data types and typical application domains. Most importantly, these surveys do not focus on 3D segmentation but give a general survey of deep learning from point clouds Guo et al. (2020), Liu et al. (2019a), Bello et al. (2020), Naseer et al. (2018), Ioannidou et al. (2017). Given the importance of the three segmentation tasks, this paper focuses exclusively on deep learning techniques for 3D segmentation. The contributions of this paper are summarized as follows:

- To the best of our knowledge, this is the first survey paper to comprehensively cover deep learning methods on 3D segmentation covering all 3D data representations, including RGB-D, projected images, voxels, point clouds, meshes, and 3D videos.
- This survey provides an in-depth analysis of the relative advantages and disadvantages of different types of 3D data segmentation methods.
- Unlike existing reviews, this survey papers focuses on deep learning methods designed specifically for 3D segmentation and also discusses typical segmentation pipelines as well as application domains.
- Finally, this survey provides comprehensive comparisons of existing methods on several public benchmark 3D datasets, draw interesting conclusions and identify promising future research directions.

Figure 2 shows a snapshot of how this survey is organized. Section 2 introduces some terminology and background concepts, including popular 3D datasets and evaluation metrics for 3D segmentation. Section 3 reviews methods for 3D semantic segmentation whereas Section 4 reviews methods for 3D instance segmentation. Section 5 provides a survey of existing methods for 3D part segmentation. Section 6 reviews the 3D segmentation methods used in some common application areas including 3D video segmentation and 3D semantic map. Section 7 presents performance comparison between 3D segmentation methods on several popular datasets, and gives corresponding data analysis. Finally, Section 8 identifies promising future research directions and concludes the paper.

2. Terminology and Background Concept

This section introduces some terminologies and background concepts, including 3D data representation, popular 3D segmentation datasets and evaluation metrics to help the reader easily navigate through the field of 3D segmentation.

2.1. 3D Segmentation Dataset

Datasets are critical to train and test 3D segmentation algorithms using deep learning. However, it is cumbersome and expensive to privately gather and annotate datasets as it needs domain expertise, high quality sensors and processing equipment. Thus, building on public datasets is an ideal way to reduce the cost. Following this way has another advantage for the community that it provides a fair comparison between algorithms. Table 1 summarizes some of the most popular and typical datasets with respect to the sensor type, data size and format, scene class and annotation method.

These datasets are acquired for 3D semantic segmentation by different type of sensors, including RGB-D cameras

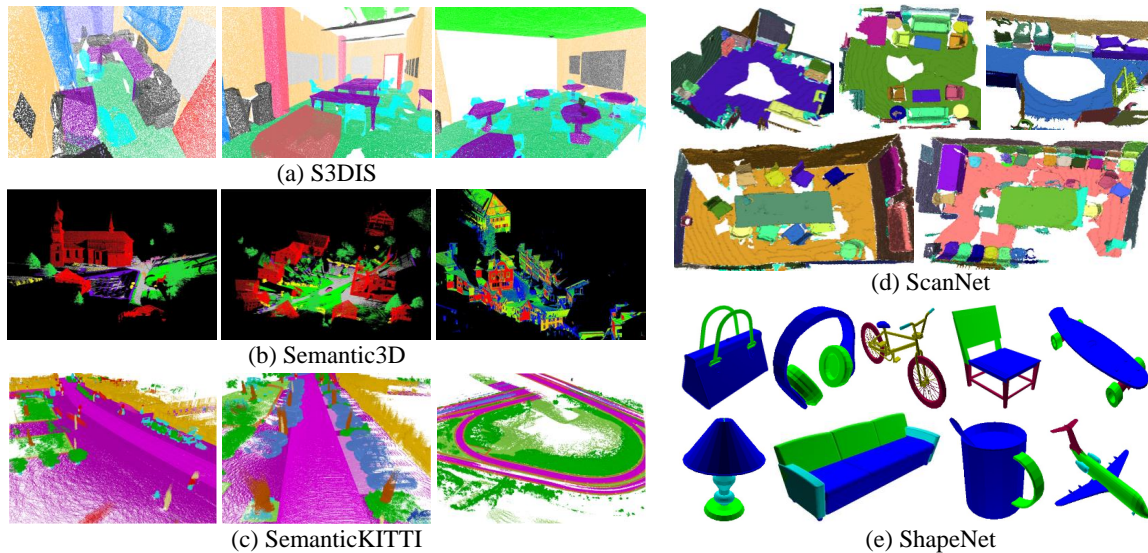


Fig. 3: Annotated examples from (a) S3DIS, (b) Semantic3D, (c) SemanticKITTI for 3D semantic segmentation, (d) ScanNet for 3D instance segmentation, and (e) ShapeNet for 3D part segmentation. See Table 1 for a summary of these datasets.

Silberman and Fergus (2011), Silberman, Hoiem, Kohli and Fergus (2012), Song, Lichtenberg and Xiao (2015), Hua, Pham, Nguyen, Tran, Yu and Yeung (2016), Dai, Chang, Savva, Halber, Funkhouser and Nießner (2017), mobile laser scanner Roynard, Deschaud and Goulette (2018), Behley, Garbade, Milioto, Quenzel, Behnke, Stachniss and Gall (2019), static terrestrial scanner Hackel, Savinov, Ladicky, Wegner, Schindler and Pollefeys (2017) and unreal engine Brodeur, Perez, Anand, Golemo, Celotti, Strub, Rouat, Larochelle and Courville (2017), Wu, Wu, Gkioxari and Tian (2018b) and other 3D scanners Armeni, Sener, Zamir, Jiang, Brilakis, Fischer and Savarese (2016), Chang, Dai, Funkhouser, Halber, Niebner, Savva, Song, Zeng and Zhang (2017). Among these, the ones obtained from unreal engine are synthetic datasets Brodeur et al. (2017) Wu et al. (2018b) that do not require expensive equipment or annotation time. These are also rich in categories and quantities of objects. Synthetic datasets have complete 360 degree 3D objects with no occlusion effects or noise compared to the real-world datasets which are noisy and contain occlusions Silberman and Fergus (2011), Silberman et al. (2012), Song et al. (2015), Hua et al. (2016), Dai et al. (2017), Roynard et al. (2018), Behley et al. (2019), Armeni et al. (2016), Hackel et al. (2017), Chang et al. (2017). For *3D instance segmentation*, there are limited 3D datasets, such as ScanNet Dai et al. (2017) and S3DIS Armeni et al. (2016). These two datasets contain scans of real-world indoor scenes obtained by RGB-D cameras or Matterport separately. For *3D part segmentation*, the Princeton Segmentation Benchmark (PSB) Chen, Golovinskiy and Funkhouser (2009), COSEG Wang, Asafi, Van Kaick, Zhang, Cohen-Or and Chen (2012) and ShapeNet Yi, Kim, Ceylan, Shen, Yan, Su, Lu, Huang, Sheffer and Guibas (2016) are three of the most popular datasets. Below, we introduce five famous segmentation datasets in detail, including S3DIS Armeni et al. (2016),

ScanNet Dai et al. (2017), Semantic3D Hackel et al. (2017), SemanticKITTI Chang et al. (2017) and ShapeNet Yi et al. (2016). Some examples with annotation from these datasets are shown in Figure 3.

S3DIS: In this dataset, the complete point clouds are obtained without any manual intervention using the Matterport scanner. The dataset consists of 271 rooms belonging to 6 large-scale indoor scenes from 3 different buildings (total of 6020 square meters). These areas mainly include offices, educational and exhibition spaces, and conference rooms etc.

Semantic3D comprises a total of around 4 billion 3D points acquired with static terrestrial laser scanners, covering up to 160×240×30 meters in real-world 3D space. Point clouds belong to 8 classes (e.g. urban and rural) and contain 3D coordinates, RGB information, and intensity. Unlike 2D annotation strategies, 3D data labeling is easily amenable to over-segmentation where each point is individually assigned to a class label.

SemanticKITTI is a large outdoor dataset containing detailed point-wise annotation of 28 classes. Building on the KITTI vision benchmark Geiger, Lenz and Urtasun (2012), SemanticKITTI contains annotations of all 22 sequences of this benchmark consisting of 43K scans. Moreover, the dataset contains labels for the complete horizontal 360 filed-of-view of the rotating laser sensor.

ScanNet dataset is particularly valuable for research in scene understanding as its annotations contain estimated calibration parameters, camera poses, 3D surface reconstruction, textured meshes, dense object level semantic segmentation, and CAD models. The dataset comprises annotated RGB-D scans of real-world environments. There are 2.5M RGB-D images in 1513 scans acquired in 707 distinct places. After RGB-D image processing, annotation human intelligence tasks were performed using the Amazon Mechanical Turk.

Table 1

Summary of popular datasets for 3D segmentation datasets including the sensor, type, size, object class, number of classes (shown in brackets), and annotation method. S←synthetic environment. R←real-world environment. Kf←thousand frames. s←scan. Mp←million points. the symbol ‘-’ means information unavailable.

Dataset	Sensors	Type	Size	Scene class (number)	Annotation method
Datasets for 3D semantic segmentation					
NYUv1 Silberman and Fergus (2011)	Microsoft Kinect v1	R	2347f	bedroom, cafe, kitchen, etc. (7)	Condition Random Field-based model
NYUv2 Silberman et al. (2012)	Microsoft Kinect v1	R	1449f	bedroom, cafe, kitchen, etc. (26)	2D annotation from AMK
SUN RGB-D Song et al. (2015)	RealSense, Xtion LIVE PRO, MKv1/2	R	10355f	objects, room layouts, etc.(47)	2D/3Dpolygons +3D bounding box
SceneNN Hua et al. (2016)	Asus Xtion PRO, MK v2	R	100s	bedroom, office, apartment, etc.(-)	3D Labels project to 2D frames
RueMonge2014 Riemenschneider, Bódis-Szomorú, Weissenberg and – Van Gool (2014)		R	428s	window, wall, balcony, door, etc(7)	Multi-view semantic labelling + CRF
ScanNet Dai et al. (2017)	Occipital structure sensor	R	2.5Mf	office, apartment, bathroom, etc(19)	3D labels project to 2D frames
S3DIS Armeni et al. (2016)	Matterport camera	R	70496f	conference rooms, offices, etc(11)	Hierarchical labeling
Semantic3D Hackel et al. (2017)	Terrestrial laser scanner	R	1660Mp	farms, town hall, sport fields, etc (8)	Three baseline methods
NPM3D Roynard et al. (2018)	Velodyne HDL-32E LiDAR	R	143.1Mp	ground, vehicle, hunman, etc (50)	Human labeling
SemanticKITTI Behley et al. (2019)	Velodyne HDL-64E	R	43Ks	ground, vehicle, hunman, etc(28)	Multi-scans semantic labelling
Matterport3D Chang et al. (2017)	Matterport camera	R	194.4Kf	various rooms (90)	Hierarchical labeling
HoME Brodeur et al. (2017)	Planner5D platform	S	45622f	rooms, object and etc.(84)	SSCNet+ a short text description
House3D Wu et al. (2018b)	Planner5D platform	S	45622f	rooms, object and etc.(84)	SSCNet+3 ways
Datasets for 3D instance segmentation					
ScanNet Dai et al. (2017)	Occipital structure sensor	R	2.5Mf	office, apartment, bathroom, etc(19)	3D labels project to 2D frames
S3DIS Armeni et al. (2016)	Matterport camera	R	70496f	conference rooms, offices, etc(11)	Active learning method
Datasets for 3D part segmentation					
ShapeNet Yi et al. (2016)	–	S	31963s	transportation, tool, etc.(16)	Propagating human label to shapes
PSB Chen et al. (2009)	Amazon’s Mechanical Turk	S	380s	human,cup, glasses airplane,etc(19)	Interactive segmentation tool
COSEG Wang et al. (2012)	–	S	1090s	vase, lamp, guiter, etc (11)	semi-supervised learning method

ShapeNet dataset has a novel scalable method for efficient and accurate geometric annotation of massive 3D shape collections. The novel technical innovations explicitly model and lessen the human cost of the annotation effort. Researchers create detailed point-wise labeling of 31963 models in shape categories in ShapeNetCore and combine feature-based classifiers, point-to-point correspondences, and shape-to-shape similarities into a single CRF optimization over the network of shapes.

2.2. Evaluation Metrics

Different evaluation metrics can assert the validity and superiority of segmentation methods including the execution time, memory footprint and accuracy. However, few authors provide detailed information about the execution time and memory footprint of their method. This paper introduces the accuracy metrics mainly.

For *3D semantic segmentation*, Overall Accuracy (OAcc), mean class Accuracy (mAcc) and mean class Intersection over Union (mIoU) are the most frequently used metrics to measure the accuracy of segmentation methods. For the sake of explanation, we assume that there are a total of $K + 1$ classes, and p_{ij} is the minimum unit (e.g. pixel, voxel, mesh, point) of class i implied to belong to class j . In other words, p_{ii} represents true positives, while p_{ij} and p_{ji} represent false positives and false negatives respectively.

Overall Accuracy is a simple metric that computes the ratio between the number of truly classified samples and the total number of samples.

$$OAcc = \sum_{i=0}^K \frac{p_{ii}}{\sum_{j=0}^K p_{ij}}$$

Mean Accuracy is an extension of OAcc, computing OAcc in a per-class and then averaging over the total number of classes K .

$$mAcc = \frac{1}{K + 1} \sum_{i=0}^K \frac{p_{ii}}{\sum_{j=0}^K p_{ij}}$$

Mean Intersection over Union is a standard metric for semantic segmentation. It computes the intersection ratio between ground truth and predicted value averaged over the total number of classes K .

$$mIoU = \frac{1}{K + 1} \sum_{i=0}^K \frac{p_{ii}}{\sum_{j=0}^K p_{ij} + \sum_{i=0}^K p_{ji} - p_{ii}}$$

For *3D instance segmentation*, Average Precision (AP) and mean class Average Precision (mAP) are also frequently used. Assuming $L_I, I \in [0, K]$ instance in every class, and c_{ij} is the amount of point of instance i inferred to belong to instance j ($i = j$ represents correct and $i \neq j$ represents incorrect segmentations).

Average Precision is another simple metric for segmentation that computes the ratio between true positives and the total number of positive samples.

$$AP = \sum_{I=0}^K \sum_{i=0}^{L_I} \frac{c_{ii}}{c_{ii} + \sum_{j=0}^{L_I} c_{ij}}$$

Mean Average precision is an extension of AP which computes per-class AP and then averages over the total

number of classes K .

$$mAP = \frac{1}{K+1} \sum_{I=0}^K \sum_{i=0}^{L_I} \frac{c_{ii}}{c_{ii} + \sum_{j=0}^{L_I} c_{ij}}$$

For *3D part segmentation*, overall average category Intersection over Union ($mIoU_{cat}$) and overall average instance Intersection over Union ($mIoU_{ins}$) are most frequently used. For the sake of explanation, we assume $M_J, J \in [0, L_I]$ parts in every instance, and q_{ij} as the total number of points in part i inferred to belong to part j . Hence, q_{ii} represents the number of true positive, while q_{ij} and q_{ji} are false positives and false negative respectively.

Overall average category Intersection over Union is an evaluation metric for part segmentation that measures the mean IoU averaged across K classes.

$$mIoU_{cat} = \frac{1}{K+1} \sum_{I=0}^K \sum_{J=0}^{L_I} \sum_{i=0}^{M_J} \frac{q_{ii}}{\sum_{j=0}^{M_J} q_{ij} + \sum_{i=0}^{M_J} q_{ji} - q_{ii}}$$

Overall average instance Intersection over Union, for part segmentation, measures the mean IoU across all instances.

$$mIoU_{ins} = \frac{1}{\sum_{I=0}^K L_I + 1} \sum_{I=0}^K \sum_{J=0}^{L_I} \sum_{i=0}^{M_J} \frac{q_{ii}}{\sum_{j=0}^{M_J} q_{ij} + \sum_{i=0}^{M_J} q_{ji} - q_{ii}}$$

3. 3D Semantic segmentation

Many deep learning methods on 3D semantic segmentation have been proposed in the literature. These methods can be divided into five categories according to the data representation used, namely, RGB-D image based, projected images based, voxel based, point based, 3D video and other representations based. Point based methods can be further categorized, based on the network architecture, into Multiple Layer Perceptron (MLP) based, Point Convolution based and Graph Convolution based and Point Transformer based methods. Figure 4 shows the milestones of deep learning on 3D semantic segmentation in recent years.

3.1. RGB-D Based

The depth map in an RGB-D image contains geometric information about the real-world which is useful to distinguish foreground objects from background, hence providing opportunities to improve the segmentation accuracy. In this category, generally the classical two-channel network is used to extract features from RGB and depth images separately. However, this simple framework is not powerful enough to extract rich and refined features. To this end, researchers have integrated several additional modules into the above simple two-channel framework to improve the performance by learning rich *context* and *geometric* information that are crucial for semantic segmentation. These modules can be roughly divided into six categories: multi-task learning, depth encoding, multi-scale network, novel neural network architectures, data/feature/score level fusion

and post-processing (see Figure 5). RGB-D image based semantic segmentation methods are summarized in Table 2. **Multi-tasks learning:** *Depth estimation* and semantic segmentation are two fundamental challenging tasks in computer vision. These tasks are also somewhat related as depth variation within an object is small compared to depth variation between different objects. Hence, many researchers choose to unite depth estimation task and semantic segmentation task. From the view of relationship of the two tasks, there are two main types of multi-task learning framework, cascade and parallel framework.

As for the cascade framework, depth estimation task provides depth images for semantic segmentation task. For example, Cao et al. [Cao, Shen and Shen \(2016\)](#) used the deep convolutional neural fields (DCNF) introduced by Liu et al. [Liu, Shen, Lin and Reid \(2015\)](#) for depth estimation. The estimated depth images and RGB images are fed into a two-channel FCN for semantic segmentation. Similarly, Guo et al. [Guo and Chen \(2018\)](#) adopted the deep network proposed by Ivanecky [Ivanecky \(2016\)](#) for automatic generating depth images from single RGB images, and then proposed a two-channel FCN model on the image pair of RGB and predicted depth map for pixel labeling.

The cascade framework performs depth estimation and semantic segmentation separately, which is simultaneously unable to perform end-to-end training for two tasks. Consequently, depth estimation task does not get any benefit from semantic segmentation task. In contrast, the *parallel* framework performs these two tasks in an unify network, which allows two tasks get benefits each other. For instance, Wang et al. [Wang, Shen, Lin, Cohen, Price and Yuille \(2015\)](#) used Joint Global CNN to exploit pixel-wise depth values and semantic labels from RGB images to provide accurate global scale and semantic guidance. As well as, they use Joint Region CNN to extract region-wise depth values and semantic map from RGB to learn detailed depth and semantic boundaries. Mousavian et al. [Mousavian, Pirsivash and Košecká \(2016\)](#) presented a multi-scale FCN comprising five streams that simultaneously explore depth and semantic features at different scales, where the two tasks share the underlying feature representation. Liu et al. [Liu, Wang, Li, Fu, Li and Lu \(2018b\)](#) proposed a collaborative deconvolutional neural network(C-DCNN) to jointly model the two tasks. However, the quality of depth maps estimated from RGB images is not as good as the one acquired directly from depth sensors. This multi-task learning pipeline has been gradually abandoned in RGB-D semantic segmentation.

Depth Encoding: Conventional 2D CNNs are unable to exploit rich geometric features from raw depth images. An alternative way is to encode raw depth images into other representations that are suitable to 2D CNN. Hoft et al. [Höft, Schulz and Behnke \(2014\)](#) used a simplified version of the histogram of oriented gradients (HOG) to represent depth channel from RGB-D scenes. Gupta et al. [Gupta, Girshick, Arbeláez and Malik \(2014\)](#) and Aman et al. [Lin, Chen, Cohen-Or, Heng and Huang \(2017\)](#) calculated three new

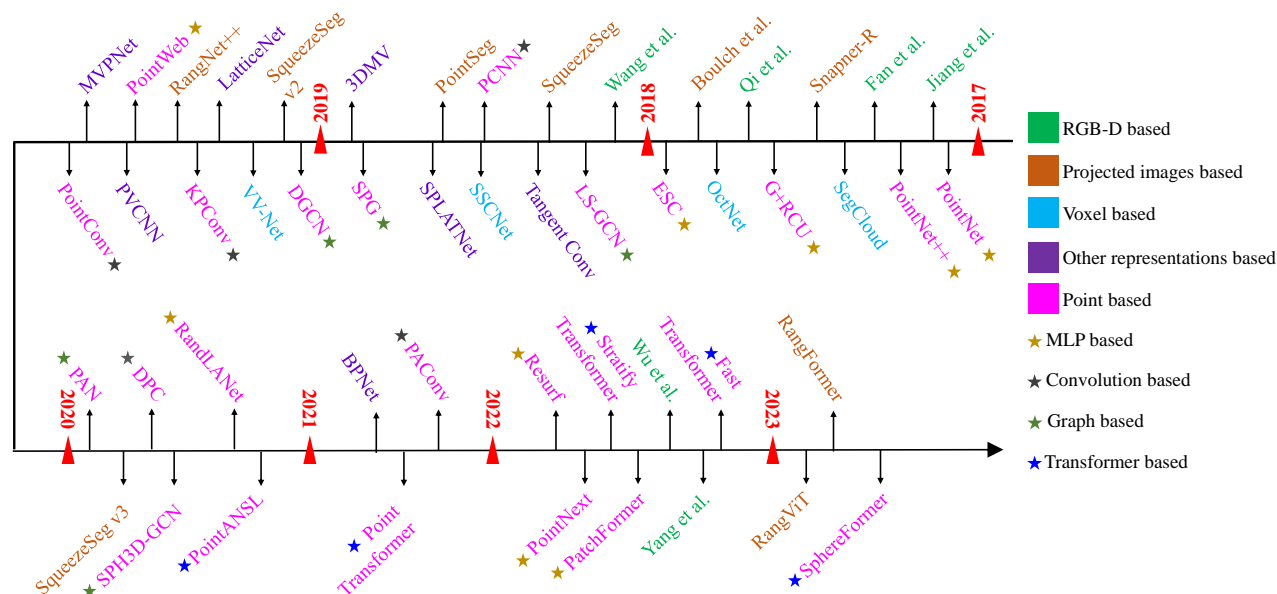


Fig. 4: Milestones of deep learning based 3D semantic segmentation methods. Note that the arrow (timeline) goes anti-clockwise

channels named horizontal disparity, height above ground and angle with gravity (HHA) from the raw depth images. Liu et al. [Liu, Wu, Wang and Qian \(2018a\)](#) point out a limitation of HHA that some scenes may not be enough horizontal and vertical planes. Hence, they propose a novel gravity direction detection method with vertical lines fitted to learn better representation. Hazirbas et al. [Hazirbas, Ma, Domokos and Cremers \(2016\)](#) also argue that HHA representation has a high computational cost and contains less information than the raw depth images. They propose an architecture called FuseNet that consists of two encoder-decoder branches, including a depth branch and an RGB branch, which directly encodes depth information with a lower computational load.

Multi-scale Network: The context information learned by multi-scale networks is useful for small objects and detailed region segmentation. Couprie et al. [Couprie, Farabet, Najman and LeCun \(2013\)](#) applied a multi-scale convolutional network to learn features directly from the RGB images and the depth images. Aman et al. [Raj, Maturana and Scherer \(2015\)](#) proposed a multi-scale deep ConvNet for segmentation where the coarse predictions of VGG16-FC net are up sampled in a Scale-2 module and then concatenated with the low-level predictions of VGG-M net in Scale-1 module to get both high and low level features. However, this method is sensitive to clutter in the scene resulting in output errors. Lin et al. [Lin et al. \(2017\)](#) exploit the fact that lower scene-resolution regions have higher depth, and higher scene-resolution regions have lower depth. They use depth maps to split the corresponding color images into multiple scene-resolution regions, and introduce context-aware receptive field (CaRF) which focuses on semantic segmentation of certain scene-resolution regions. This makes their pipeline a multi-scale network.

Novel Neural Networks: Given the fixed grid computation of CNNs, their ability to process and exploit geometric information is limited. Therefore, researchers have proposed other novel neural network architectures to better exploit geometric features and the relationships between RGB and depth images. These architectures can be divided into five main categories.

Improved 2D Convolutional Neural Networks (2D CNNs) Inspired from cascaded feature networks [Lin et al. \(2017\)](#), Jiang et al. [Jiang, Zhang, Huang and Zheng \(2017\)](#) proposed a novel Dense-Sensitive Fully Convolutional Neural Network (DFCN) which incorporates depth information into the early layers of the network using feature fusion tactics. This is followed by several dilated convolutional layers for context information exploitation. Similarly, Wang et al. [Wang and Neumann \(2018\)](#) proposed a depth-aware 2D CNN by introducing two novel layers, depth aware convolution layer and depth-aware pooling layer, which are based on the prior that pixels with the same semantic label and similar depth should have more impact on one another.

Deconvolutional Neural Networks (DeconvNets) are a simple yet effective and efficient solution for the refinement of segmentation map. Liu et al. [Liu et al. \(2018b\)](#) and Wang et al. [Wang, Wang, Tao, See and Wang \(2016\)](#) all adopt the DeconvNet for RGB-D semantic segmentation because of good performance. However, the potential of DeconvNet is limited since the high-level prediction map aggregates large context for dense prediction. To this end, Cheng et al. [Cheng, Cai, Li, Zhao and Huang \(2017\)](#) proposed a locality-sensitive DeconvNet (LS-DeconvNet) to refine the boundary segmentation over depth and color images. LS-DeconvNet incorporates local visual and geometric cues from the raw RGB-D data into each DeconvNet, which is able to up sample the coarse convolutional maps with large context while recovering sharp object boundaries.

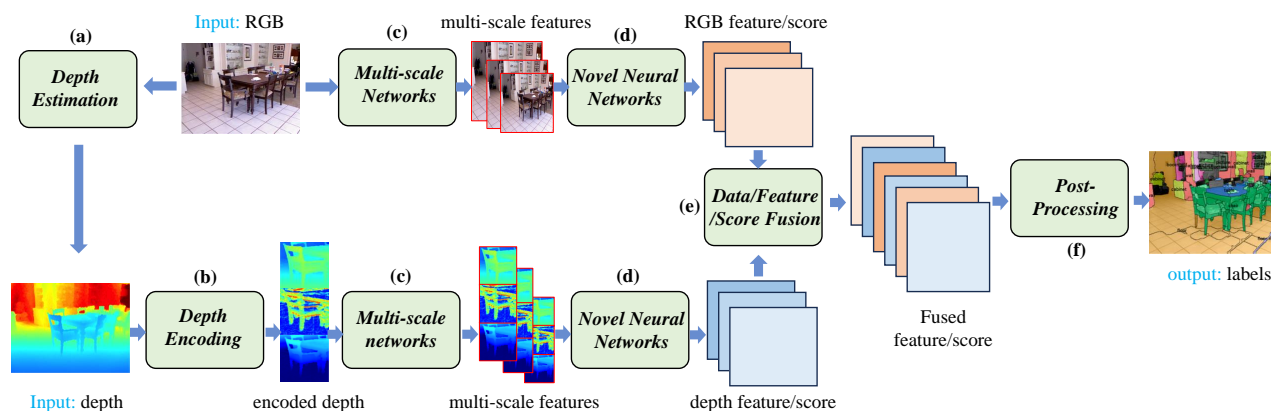


Fig. 5: Typical two-channel framework with six improvement modules, including (a) multi-tasks learning, (b) depth encoding, (c) multi-scale network, (d) novel neural network architecture, (e) feature/score level fusion, and (f) post-processing.

Recurrent Neural Networks (RNNs) can capture long-range dependencies between pixels but are mainly suited to a single data channel (e.g. RGB). Fan et al. [Fan, Mei, Prokhorov and Ling \(2017\)](#) extended the single-modal RNNs to multimodal RNNs (MM-RNNs) for application to RGB-D scene labeling. The MM-RNNs allow ‘memory’ sharing across depth and color channels. Each channel not only possess its own features but also has the attributes of other channel making the learned features more discriminative for semantic segmentation. Li et al. [Li, Gan, Liang, Yu, Cheng and Lin \(2016\)](#) proposed a novel Long Short-Term Memorized Context Fusion (LSTM-CF) model to capture and fuse contextual information from multiple channels of RGB and depth images.

Graph Neural Networks (GNNs) were first used for RGB-D semantic segmentation by Qi et al. [Qi, Liao, Jia, Fidler and Urtasun \(2017c\)](#) who cast the 2D RGB pixels into 3D space based on depth information and associated the 3D points with semantic information. Next, they built a k-nearest neighbor graph from the 3D points and applied a 3D graph neural network (3DGNN) to perform pixelwise predictions.

Transformers have gained popularity in RGB image segmentation and have also been extended to RGB-D segmentation. Researchers have proposed various approaches to leverage Transformers for this purpose. One notable work by Ying et al. [Ying and Chuah \(2022\)](#) introduces the concept of Uncertainty-Aware Self-Attention, which explicitly manages the information flow from unreliable depth pixels to confident depth pixels during feature extraction. This approach aims to address the challenges posed by noisy or uncertain depth information in RGB-D segmentation. Another study by Wu et al. [Wu, Zhou, Allibert, Stolz, Démonceaux and Ma \(2022c\)](#) adopts the Swin-Transformer directly to exploit both the RGB and depth features. By leveraging the self-attention mechanism, this approach captures long-range dependencies and enables effective fusion of RGB and depth information for segmentation. Inspired by the success of the Swin-Transformer, Yang et al. [Yang, Xu, Zhang, Xu and Huang \(2022\)](#) proposes a hierarchical Swin-RGBD

Transformer. This model incorporates and leverages depth information to complement and enhance the ambiguous and obscured features in RGB images. The hierarchical architecture allows for multi-scale feature learning and enables more effective integration of RGB and depth information.

Data/Feature/Score Fusion: Optimal fusion of the texture (RGB channels) and geometric (depth channel) information is important for accurate semantic segmentation. There are three fusion tactics: data level, feature level and score level, referring to early, middle and late fusion respectively. A simple *data level fusion* strategy is to concatenate the RGB and depth images into four channels for direct input to a CNN model e.g. as performed by Couprie et al. [Couprie et al. \(2013\)](#). However, such a data level fusion does not exploit the strong correlations between depth and photometric channels. *Feature level fusion*, on the other hand, captures these correlations. For example, Li et al. [Li et al. \(2016\)](#) proposed a memorized fusion layer to adaptively fuse vertical depth and RGB contexts in a data-driven manner. Their method performs bidirectional propagation along the horizontal direction to hold true 2D global contexts. Similarly, Wang et al. [Wang et al. \(2016\)](#) proposed a feature transformation network that correlates the depth and color channels, and bridges the convolutional networks and deconvolutional networks in a single channel. The feature transformation network can discover specific features in a single channel as well as common features between two channels, allowing the two branches to share features to improve the representation power of shared information. The above complex feature level fusion models are inserted in a specific same layer between RGB and depth channels, which is difficult to train and ignores other same layer feature fusion. To this end, Hazirbas et al. [Hazirbas et al. \(2016\)](#) and Jiang et al. [Jiang et al. \(2017\)](#) carry out fusion as an element-wise summation to fuse feature of multiple same layers between the two channels. Wu et al. [Wu et al. \(2022c\)](#) propose a novel Transformer-based fusion scheme, named TransD-Fusion to better model long-range contextual information.

Table 2

Summary of RGB-D based methods with deep learning. Est.←depth estimation. Enc.←depth encoding. Mul.←multi-scale networks. Nov.←novel neural networks. Fus.←data/feature/score fusion. Pos.←post-processing.

Methods	Est.	Enc.	Mul.	Nov.	Fus.	Pos.	Architecture(2-stream)	Contribution
Cao et al. (2016)	✓	✓	×	×	✓	×	FCNs	Estimating depth images+a unified network for two tasks
Guo and Chen (2018)	✓	×	×	×	✓	×	FCNs	Incorporating depth & gradient for depth estim.
Wang et al. (2015)	✓	×	×	×	×	✓	Region./Global CNN	HCRF for fusion and refining + two tasks by a network
Mousavian et al. (2016)	✓	×	✓	×	✓	✓	FCN	FC-CRF for refining + Mutual improvement for two tasks
Liu et al. (2018b)	✓	×	×	✓	×	✓	S/D-DCNN	PBL for two feature maps integration + FC-CRF
Höft et al. (2014)	×	✓	×	×	×	×	CNNs	A embedding for depth images
Gupta et al. (2014)	×	✓	×	×	×	×	CNNs	HHA for depth images
Liu et al. (2018a)	×	✓	×	×	✓	✓	DCNNs	New depth encoding+ FC-CRF for refining
Hazirbas et al. (2016)	×	✓	×	×	✓	×	Encoder-decoder	Semantic and depth feature fusion at each layer
Coupric et al. (2013)	×	×	✓	×	✓	×	ConvNets	RGB laplacian pyramid for multi-scale features
Raj et al. (2015)	×	✓	✓	×	✓	×	VGG-M	New multi-scale deep CNN
Lin et al. (2017)	×	×	✓	✓	✓	×	CFN	CaRF for multi-resolution features
Jiang et al. (2017)	×	×	×	✓	✓	✓	RGB-FCN	Semantic & depth feature fusion at each layer + DCRF
Wang and Neumann (2018)	×	×	×	✓	×	×	Depth-aware CNN	Depth-aware Conv. and depth aware average pooling
Cheng et al. (2017)	×	✓	×	✓	✓	×	FCN + Deconv	LS-DeconvNet + novel gated fusion
Fan et al. (2017)	×	×	×	✓	✓	×	MM-RNNs	Multimodal RNN
Li et al. (2016)	×	✓	×	✓	✓	×	LSTM-CF	LSTM-CF for capturing and fusing contextual inf.
Qi et al. (2017c)	×	×	×	✓	×	×	3DGN	GNN for RGB-D semantic segmentation
Wang et al. (2016)	×	×	×	✓	✓	×	ConvNet-DeconvNet	MK-MMD for assessing the similarity between common features
Ying and Chuah (2022)	×	×	×	✓	✓	×	Swin-Transformer	Effective and scalable fusion module based on cross-attention
Wu et al. (2022c)	×	×	×	✓	✓	×	Swin-Transformers	Transformer-based fusion module
Yang et al. (2022)	×	×	×	✓	×	×	Swin-Transformer+ResNet	Swin-RGB-D Transformer

Score level fusion is commonly performed using the simple averaging strategy. However, the contributions of RGB model and depth model for semantic segmentation are different. Liu et al. Liu et al. (2018a) proposed a score level fusion layer with weighted summation that uses a convolution layer to learn the weights from the two channels. Similarly, Cheng et al. Cheng et al. (2017) proposed a gated fusion layer to learn the varying performance of RGB and depth channels for different class recognition in different scenes. Both techniques improved the results over the simple averaging strategy at the cost of additional learnable parameters.

Post-Processing: The results of CNN or DCNN used for RGB-D semantic segmentation are generally very coarse resulting in rough boundaries and the vanishing of small objects. A common method to address this problem is to couple the CNN with a Conditional Random Field (CRF). Wang et al. Wang et al. (2015) further boost the mutual interactions between the two channels by the joint inference of Hierarchical CRF (HCRF). It enforces synergy between global and local predictions, where the global layouts are used to guide the local predictions and reduce local ambiguities, as well as local results provide detailed regional structures and boundaries. Mousavian et al. Mousavian et al. (2016), Liu et al. Liu et al. (2018b), and Long et al. Liu et al. (2018a) adopt a Fully Connected CRF (FC-CRF) for post-processing, where the pixel-wise label prediction jointly considers geometric constraint, such as pixel-wise normal information, pixel position, intensity and depth, to promote the consistency of pixel-wise labeling. Similarly, Jiang et al. Jiang et al. (2017) proposed Dense-sensitive CRF (DCRF) that integrates the depth information with FC-CRF.

3.2. Projected Images Based Segmentation

The core idea of projected images based semantic segmentation is to use 2D CNNs to exploit features from projected images of 3D scenes/shapes and then fuse these features for label prediction. This pipeline not only exploits more semantic information from large-scale scenes compared to a single-view image, but also reduces the data size of a 3D scene compared to a point cloud. The projected images mainly include *multi-view images* or *spherical images*.

Among, multi-view images projection is usually employed on RGB-D datasets Dai et al. (2017), and statics terrestrial scanning datasets Hackel et al. (2017). Spherical images projection is usually employed on self-driving mobile laser scanning datasets Behley et al. (2019). Projected images based semantic segmentation methods are summarized in Table 3.

3.2.1. Multi-View Images Based Segmentation

MVCNN Su, Maji, Kalogerakis and Learned-Miller (2015) uses a unified network to combine features from multiple views of a 3D shape, formed by a virtual camera, into a single and compact shape descriptor to get improved classification performance. This inspired researchers to take the same idea into 3D semantic segmentation (see Figure 6). For example, Lawin et al. Lawin, Danelljan, Tosteborg, Bhat, Khan and Felsberg (2017) project point clouds into multi-view synthetic images, including RGB, depth and surface normal images. The prediction score of all multi-view images is fused into a single representation and back-projected into each point. However, the snapshot can erroneously catch the points behind the observed structure if the density of the point cloud is low, which makes the deep network to misinterpret the multiple views. To this end,

SnapNet [Boulch, Le Saux and Audebert \(2017\)](#), [Boulch, Guerry, Le Saux and Audebert \(2018\)](#) preprocesses point clouds for computing point features (like normal or local noise) and generating a mesh, which is similar to point cloud densification. From the mesh and point clouds, they generate RGB and depth images by suitable snapshot. Then, they perform a pixel-wise labeling of 2D snapshots using FCN and fast back-project these labels into 3D points by efficient buffering. Above methods need obtain the whole point clouds of 3D scene in advance to provide a complete spatial structure for back-projection. However, the multi-view images directly obtained from real-world scene would lose much spatial information. Some works attempt to unite 3D scene reconstruction with semantic segmentation, where scene reconstruction could make up for spatial information. For example, [Guerry et al. Guerry, Boulch, Le Saux, Moras, Plyer and Filliat \(2017\)](#) reconstruct 3D scene with global multi-view RGB and Gray stereo images. Then, the labels of 2D snapshots are back-projected onto the reconstructed scene. But, simple back-projection can not optimally fuse semantic and spatial geometric features. Along the line, [Pham et al. Pham, Hua, Nguyen and Yeung \(2019a\)](#) proposed a novel Higher-order CRF, following back-projection, to further develop the initial segmentation.

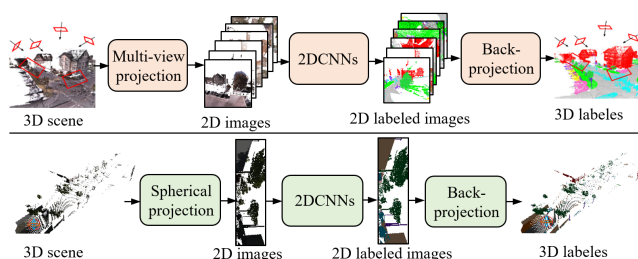


Fig. 6: Illustration of basic frameworks for projected images based segmentation methods. **Top:** Multi-view images based framework. **Bottom:** Spherical images based framework.

3.2.2. Spherical Images Based Segmentation

Selecting snapshots from a 3D scene is not straight forward. Snapshots must be taken after giving due consideration to the number of viewpoints, viewing distance and angle of the virtual cameras to get an optimal representation of the complete scene. To avoid these complexities, researchers project the complete point cloud onto a sphere (see Figure 6.Bottom). For example, [Wu, Wan, Yue and Keutzer \(2018a\)](#) proposed an end-to-end pipeline called SqueezeSeg, inspired from SqueezeNet [Iandola, Han, Moskewicz, Ashraf, Dally and Keutzer \(2016\)](#), to learn features from spherical images which are then refined by CRF implemented as a recurrent layer. Similarly, [PointSeg Wang, Shi, Yun, Tai and Liu \(2018e\)](#) extends the SqueezeNet by integrating the feature-wise and channel-wise attention to learn robust representation. [SqueezeSegv2 Wu, Zhou, Zhao, Yue and Keutzer \(2019a\)](#) improves the structure of SqueezeSeg with Context Aggregation Module (CAM), adding LiDAR mask as a channel to increase robustness to noise.

[RangNet++ Milioto, Vizzo, Behley and Stachniss \(2019\)](#) transfers the semantic labels to 3D point clouds, avoiding discarding points regardless of the level of discretization used in CNN. Despite the likeness between regular RGB and LiDAR images, the feature distribution of LiDAR images changes at different locations. [SqueezeSegv3 Xu, Wu, Wang, Zhan, Vajda, Keutzer and Tomizuka \(2020\)](#) has a spatially-adaptive and context-aware convolution, termed Spatially-Adaptive Convolution (SAC) to adopt different filters for different locations. Inspired by the success of 2D vision Transformer, [RangViT Ando, Gidaris, Bursuc, Puy, Boulch and Marlet \(2023\)](#) leverage ViTs pre-trained on long natural image datasets by adding the down and up module on the top and bottom of ViTs, and achieves a good performance comparing to the projection based methods. Similarly, to make the long projection image to suit the ViTs, [RangeFormer Kong, Liu, Chen, Ma, Zhu, Li, Hou, Qiao and Liu \(2023\)](#) adopts a scalable training strategy that splits the whole projection image into several sub-images, and puts them into ViTs for training. After training, the predictions are merged sequentially to form the complete scene.

3.3. Voxel Based Segmentation

Similar to pixels, voxels divide the 3D space into many volumetric grids with a specific size and discrete coordinates. It contains more geometric information of the scene compared to projected images. 3D ShapeNets [Wu, Song, Khosla, Yu, Zhang, Tang and Xiao \(2015\)](#) and VoxNet [Maturana and Scherer \(2015\)](#) take volumetric occupancy grid representation as input to a 3D convolutional neural network for object recognition, which guides 3D semantic segmentation based on voxels. Voxel based semantic segmentation methods are summarized in Table 3.

3D CNN is a common architecture used to process uniform voxels for label prediction. [Huang et al. Huang and You \(2016\)](#) presented a 3D FCN for coarse voxel level predictions. Their method is limited by spatial inconsistency between predictions and provide a coarse labeling. [Tchapmi et al. Tchapmi et al. \(2017\)](#) introduce a novel network SEG-Cloud to produce fine-grained predictions. It up samples the coarse voxel-wise prediction obtained from a 3D FCN to the original 3D point space resolution by trilinear interpolation.

With fixed resolution voxels, the computational complexity grows linearly with the increase of the scene scale. Large voxels can lower the computational cost of large-scale scene parsing. [Liu et al. Liu et al. \(2017\)](#) introduced a novel network called 3D CNN-DQN-RNN. Like the sliding windows in 2D semantic segmentation, this network proposes eye window that traverses the whole data for fast localizing and segmenting class objects under the control of 3D CNN and deep Q-Network (DQN). The 3D CNN and Residual RNN further refine features in the eye window. The pipeline learns key features of interesting regions efficiently to enhance the accuracy of large-scale scene parsing with less computational cost. [Rethage et al. Rethage et al. \(2018\)](#) present a novel fully convolutional point network (FCPN), sensitive to multi-scale input, to parse large-scale scene

Table 3

Summary of projected images/voxel/other representation based methods with deep learning. M←multi-view image. S←spherical image. V←voxel. T←tangent images. L←lattice. P←point clouds.

Type	Methods	Input	Architecture	Feature extractor	Contribution
projection	Lawin et al. Lawin et al. (2017)	M	multi-stream	VGG-16	Investigate the impact of different input modalities
	Boulch et al. Boulch et al. (2017) Boulch et al. (2018)	M	SegNet/U-Net	VGG-16	New and efficient framework SnapNet
	Guerry et al. Guerry et al. (2017)	M	SegNet/U-Net	VGG-16	Improved MVCNN+3D consistent data augment.
	Pham et al. Pham et al. (2019a)	M	Two-stream	2DConv	High-order CRF+ real-time reconstruction pipeline
	Wu et al. Wu et al. (2018a)	S	AlexNet	Firemodules	End-to-end pipeline SqueezeSeg + real time
	Wang et al. Wang et al. (2018e)	S	AlexNet	Firemodules	Quite light-weight framework PointSeg + real time
	Wu et al. Wu et al. (2019a)	S	AlexNet	Firemodules	Robust framework SqueezeSegV2
	Milioto et al. Milioto et al. (2019)	S	DarkNet	Residual block	GPU-accelerated post-processing + RangNet++
	Xu et al. Xu et al. (2020)	S	RangeNet	SAC	Adopting different filters for different locations
	Ando et al. Ando et al. (2023)	S	U-Net	ViTs	Decreasing the gaps between image and point domain.
Kong et al. Kong et al. (2023)	S	U-Net	ViTs	Introducing a scalable training from range view strategy	
voxel	Huang et al. Huang and You (2016)	V	3D CNN	3DConv	Efficiently handling large data
	Tchapmi et al. Tchapmi, Choy, Armeni, Gwak and Savarese (2017)	V	3D FCNN	3DConv	Combining 3D FCNN with fine-represen.
	Meng et al. Meng, Gao, Lai and Manocha (2019)	V	VAE	RBF	A novel voxel-based representation + RBF
	Liu et al. Liu, Li, Zhang, Zhou, Ye, Wang and Lu (2017)	V	3D CNN/DQN/RNN	3DConv	Integrating three vision tasks into one frame.
	Rethage et al. Rethage, Wald, Sturm, Navab and Tombari (2018)	V	3D FCNN	FPConv	First fully-convolutional network on raw point sets
	Dai et al. Dai, Ritchie, Bokeloh, Reed, Sturm and Nießner (2018)	V	3D FCNN	3DConv	Combing scene completion and semantic labeling
	Riegler et al. Riegler, Osman Ulusoy and Geiger (2017)	V	Octree	3DConv	Making DL with high-resolution voxels
	Graham et al. Graham, Engelcke and Van Der Maaten (2018)	V	FCN/U-Net	SSConv	SSConv with less computation
others	TangentConv Tatarchenko, Park, Koltun and Zhou (2018)	T	U-Net	TConv	Tangent convolution + Parsing large scenes
	SPLATNet Su, Jampani, Sun, Maji, Kalogerakis, Yang and Kautz (2018)	L	DeepLab	BConv	Hierarchical and spatially-aware feature learning
	LatticeNet Rosu, Schütt, Quenzel and Behnke (2019)	L	U-Net	PN+3DConv	Hybrid architecture + novel slicing operator
	3DMV Dai and Nießner (2018)	M+V	Cascade frame.	ENet+3DConv	Inferring 3D semantics from both 3D and 2D input
	Hung et al. Chiang, Lin, Liu and Hsu (2019)	V+M+P	Parallel frame.	SSCNet/DeepLab/PN	Leveraging 2D and 3D features
	PVCNN Liu, Tang, Lin and Han (2019b)	V+P	POintNet	PVConv	Both memory and computation efficient
	MVPNet Jaritz, Gu and Su (2019)	M+P	Cascade frame.	U-Net+PointNet++	Leveraging 2D and 3D features
	LaserNet++ Meyer, Charland, Hegde, Laddha and Vallespi-Gonzalez (2019)	M+P	Cascade frame.	ResNet+LNet	Unified network for two tasks
	BPNet Hu, Zhao, Jiang, Jia and Wong (2021)	M+P	Cascade frame.	2/3DUNet	Bidirection projection module

without pro- or post-process steps. Particularly, FCPN is able to learn memory efficient representations that scale well to larger volumes. Similarly, Dai et al. [Dai et al. \(2018\)](#) design a novel 3D CNN to train on scene subvolumes but deploy on arbitrarily large scenes at test time, as it is able to handle large scenes with varying spatial extent. Additionally, their network adopts a coarse-to-fine tactic to predict multiple resolution scenes to handle the resolution growth in data size as the scene increases in size. Traditionally, the voxel representation only comprises Boolean occupancy information which loses much geometric information. Meng et al. [Meng et al. \(2019\)](#) develop a novel information-rich voxel representation by using a variational auto-encoder(VAE) taking radial basis function(RBF) to capture the distribution of points within each voxel. Further, they proposed a group equivariant convolution to exploit feature.

In fixed scale scenes, the computational complexity grows cubically as the voxel resolution increases. However, the volumetric representation is naturally sparse, resulting in unnecessary computations when applying 3D dense convolution on the sparse data. To alleviate this problem, OctNet [Riegler et al. \(2017\)](#) divides the space hierarchically into nonuniform voxels using a series of unbalanced octrees. Tree structure allows memory allocation and computation

to focus on relevant dense voxels without sacrificing resolution. However, empty space still imposes computational and memory burden in OctNet. In contrast, Graham et al. [Graham et al. \(2018\)](#) proposed a novel submanifold sparse convolution (SSC) that does not perform computations in empty regions, making up for the drawback of OctNet.

3.4. Point Based Segmentation

Point clouds are scattered irregularly in 3D space, lacking any canonical order and translation invariance, which restricts the use of conventional 2D/3D convolutional neural networks. Recently, a series of point-based semantic segmentation networks have been proposed. These methods can be roughly subdivided into four categories: MLP based, point convolution based, graph convolution based and Transformer based. These methods are summarized in Table 4.

3.4.1. MLP Based

These methods apply a Multi Layer Perceptron directly on the points to learn features. The PointNet [Qi, Su, Mo and Guibas \(2017a\)](#) is a pioneering work that directly processes point clouds. It uses shared MLP to exploit points-wise features and adopts a symmetric function such as max-pooling to collect these features into a global feature representation.

Because the max-pooling layer only captures the maximum activation across global points, PointNet cannot learn to exploit local features. Building on PointNet, PointNet++ [Qi, Yi, Su and Guibas \(2017b\)](#) defines a hierarchical learning architecture. It hierarchically samples points using farthest point sampling (FPS) and groups local regions using k nearest neighbor search as well as ball search. Progressively, a simplified PointNet exploits features in local regions at multiple scales or multiple resolutions. Similarly, Engelmann et al. [Engelmann, Kontogianni, Schult and Leibe \(2018\)](#) define local regions by KNN clustering and K-means clustering and use a simplified PointNet to extract local features.

To learn the short and long-range dependencies, some works introduce the Recurrent Neural Networks (RNN) to MLP-based methods. For example, ESC [Engelmann, Kontogianni, Hermans and Leibe \(2017\)](#) divides global points into multi-scale/grid blocks. The concatenated (local) block features are appended to the point-wise features and passed through Recurrent Consolidation Units (RCUs) to further learn global context features. Similarly, HRNN [Ye, Li, Huang, Du and Zhang \(2018\)](#) uses Pointwise Pyramid Pooling (3P) to extract local features on the multi-size local regions. Point-wise features and local features are concatenated and a two-direction hierarchical RNN explores context features on these concatenated features. However, the local features learned are not sufficient because the deeper layer features do not cover a larger spatial extent.

Another technology, some works integrate the hand-craft point representation into PointNet or PointNet++ network to enhance the point representation ability with less learnable network parameters. Inspired by SIFT representation [Lowe \(2004\)](#), PointSIFT [Jiang, Wu, Zhao, Zhao and Lu \(2018\)](#) inserts a PointSIFT module layer learn local shape information. This module transforms each point into a new shape representation by encoding information of different orientations. PointWeb [Zhao, Jiang, Fu and Jia \(2019a\)](#) propose a adaptive feature adjustment (AFA) module to learning the interactive information between local points to enhance the point representation. Similarly, RepSurf [Ran, Liu and Wang \(2022\)](#) introduces two novel point representations, namely triangular and umbrella representative surfaces, to establish connections and enhance the representation capability of learned point-wise features. This approach effectively improves feature representation with fewer learnable network parameters, drawing significant attention from the research community. In contrast to the aforementioned methods, PointNeXt [Qian, Li, Peng, Mai, Hammoud, Elhoseiny and Ghanem \(2022\)](#) takes a different approach by revisiting the classical PointNet++ architecture through a systematic study of model training and scaling strategies. It proposes a set of improved training strategies that lead to a significant performance boost for PointNet++. Additionally, PointNeXt introduces an inverted residual bottleneck design and employs separable MLPs to enable efficient and effective model scaling.

3.4.2. Point Convolution Based

Point convolution based methods perform convolution operations directly on the points. Different from 2D convolution, the weight function of point convolution need learn from point geometric information adaptively. Early convolution networks focus on the convolution weight function design. For example, RSNet [Huang, Wang and Neumann \(2018\)](#) exploit point-wise features using 1×1 convolution and then pass them through the local dependency module (LDM) to exploit local context features. However, it does not define the neighborhood for each point in order to learn local features. On the other hand, PointwiseCNN [Hua, Tran and Yeung \(2018\)](#) sorts points in a specific order, e.g. XYZ coordinate or Morton curve [Morton \(1966\)](#), and queries nearest neighbors dynamically and bins them into $3 \times 3 \times 3$ kernel cells before convolving with the same kernel weights.

Gradually, some point convolution works approximate the convolution weight function as MLP to learn weights from point coordinates. PCCN [Wang, Suo, Ma, Pokrovsky and Urtasun \(2018c\)](#) performs Parametric CNN, where the kernel is estimated as an MLP, on KD-tree neighborhood to learn local features. PointCNN [Li, Bu, Sun, Wu, Di and Chen \(2018b\)](#) coarsens the input points with farthest point sampling. The convolution layer learns an χ -transformation from local points by MLP to simultaneously weight and permute the features, subsequently applying a standard convolution on these transformed features.

Some works associates a coefficient (derived from point coordinates) with the weight function to adjust the learned convolutional weights. An extension of Monte Carlo approximation for convolution called PointConv [Wu, Qi and Fuxin \(2019b\)](#) takes the point density into account. It uses MLP to approximate a weight function of the convolution kernel, and applies an inverse density scale to reweight the learned weight function. Similarly, MCC [Hermosilla, Ritschel, Vázquez, Vinacua and Ropinski \(2018\)](#) phrases convolution as a Monte Carlo integration problem by relying on point probability density function (PDF), where the convolution kernel is also represented by an MLP. Moreover, it introduces Poisson Disk Sampling (PDS) [Wei \(2008\)](#) to construct a point hierarchy instead of FPS, which provides an opportunity to get the maximal number of samples in a receptive field.

Another line of works use other function instead of MLP to approximate the convolution weight function. Flex-Convolution [Groh, Wieschollek and Lensch \(2018\)](#) uses a linear function with fewer parameters to model a convolution kernel and adapts inverse density importance subsampling (IDISS) to coarsen the points. KPConv [Thomas, Qi, Deschaud, Marcotegui, Goulette and Guibas \(2019\)](#) and KCNet [Shen, Feng, Yang and Tian \(2018\)](#) fixed the convolution kernel for robustness to varying point density. These networks predefine the kernel points on local region and learn convolutional weights on the kernel points from their geometric connections to local points using linear and Gaussian correlation functions, respectively. Here, the number

and position of kernel points need be optimized for different datasets.

Point convolution on limited local receptive field could not exploit long-range features. Therefore, some works introduce the dilated mechanism into point convolution. Dilated point convolution (DPC) [Engelmann, Kontogianni and Leibe \(2020b\)](#) adapts standard point convolution on neighborhood points of each point where the neighborhood points are determined through a dilated KNN search. Similarly, A-CNN [Komarichev, Zhong and Hua \(2019\)](#) defines a new local ring-shaped region by dilated KNN, and projects points on a tangent plane to further order neighbor points in local regions. Then, the standard point convolutions are performed on these ordered neighbors represented as a closed loop array.

In the large-scale point clouds semantic segmentation area, RandLA-Net [Hu, Yang, Xie, Rosa, Guo, Wang, Trigoni and Markham \(2020\)](#) uses random point sampling instead of the more complex point selection approach. It introduces a novel local feature aggregation module (LFAM) to progressively increase the receptive field and effectively preserve geometric details. Another technology, PolarNet [Zhang, Zhou, David, Yue, Xi, Gong and Foroosh \(2020\)](#) first partitions a large point cloud into smaller grids (local regions) along their polar bird's-eye-view (BEV) coordinates. It then abstracts local region points into a fixed-length representation by a simplified PointNet and these representations are passed through a standard convolution.

3.4.3. Graph Convolution Based

The graph convolution based methods perform convolution on points connected with a graph structure, where the graph help the feature aggregation exploit the structure information between points. the graphs can be divided into spectral graph and spatial graph. In the *spectral graph*, LS-GCN [Wang, Samari and Siddiqi \(2018a\)](#) adopts the basic architecture of PointNet++, replaces MLPs with a spectral graph convolution using standard unparametrized Fourier kernels, as well as a novel recursive spectral cluster pooling substitute for max-pooling. However, transformation from spatial to spectral domain incurs a high computational cost. Besides that, spectral graph networks are usually defined on a fixed graph structure and are thus unable to directly process data with varying graph structures.

In the *spatial graph* category, ECC [Simonovsky and Komodakis \(2017\)](#) is among of the pioneer methods to apply spatial graph network to extract features from point clouds. It dynamically generates edge-conditioned filters to learn edge features that describe the relationships between a point and its neighbors. Based on PointNet architecture, DGCNN [Wang, Sun, Liu, Sarma, Bronstein and Solomon \(2019b\)](#) implements dynamic edge convolution called EdgeConv on the neighborhood of each point. The convolution is approximated by a simplified PointNet. SPG [Landrieu and Simonovsky \(2018\)](#) parts the point clouds into a number of simple geometrical shapes (termed super-points) and builds super graph on global super-points. Furthermore, this

network adopts PointNet to embed these points and refine the embedding by Gated Recurrent Unit (GRU). Based on the basic architecture of PointNet++, Li et al. [Li, Ma, Zhong, Cao and Li \(2019b\)](#) proposed Geometric Graph Convolution (TGCov), its filters defined as products of local point-wise features with local geometric connection features expressed by Gaussian weighted Taylor kernels. Feng et al. [Feng, Zhang, Lin, Gilani and Mian \(2020\)](#) constructed a local graph on neighborhood points searched along multi-directions and explore local features by a local attention-edge convolution (LAE-Conv). These features are imported into a point-wise spatial attention module to capture accurate and robust local geometric details. Lei et al. designs a fuzzy coefficient to times weight function, to enable the convolution weights robust.

Continuous graph convolution also incurs a high computational cost and generally suffer from the vanishing gradient problem. Inspired by the separable convolution strategy in Xception [Chollet \(2017\)](#) that significantly reduces parameters and computation burden, HDGCN [Liang, Yang, Deng, Wang and Wang \(2019a\)](#) designed a DGConv that composes depth-wise graph convolution followed by a point-wise convolution, and add DGConv into the hierarchical structure to extract local and global features. DeepGCNs [Li, Muller, Thabet and Ghanem \(2019a\)](#) borrows some concepts from 2D CNN such as residual connections between different layers (ResNet) to alleviate the vanishing gradient problem, and dilation mechanism to allow the GCN to go deeper. Lei et al. [Lei, Akhtar and Mian \(2020\)](#) propose a discrete spherical convolution kernel (SPH3D kernel) that consists of the spherical convolution learning depth-wise features and point-wise convolution learning point-wise features.

Tree structures such as KD-tree and Octree can be viewed as a special type of graph, allowing to share convolution layers depending on the tree splitting orientation. 3DContextNet [Zeng and Gevers \(2018\)](#) adopts a KD-tree structure to hierarchically represent points where the nodes of different tree layers represent local regions at different scales, and employs a simplified PointNet with a gating function on nodes to explore local features. However, their performance depends heavily on the randomization of the tree construction. Lei et al. [Lei, Akhtar and Mian \(2019\)](#) built an Octree based hierarchical structure on global points to guide the spherical convolution computation in per layer of the network. The spherical convolution kernel systematically partitions a 3D spherical region into multiple bins that specifies learnable parameters to weight the points falling within the corresponding bin.

3.4.4. Transformer Based

Attention mechanism has recently become popular for improving point cloud segmentation accuracy. Compared to point convolution, Transformer introduces the point features into the weight learning. For example, Ma et al. [Ma, Guo, Liu, Lei and Wen \(2020\)](#) use the channel self-attention mechanism to learn independence between any two point-wise feature channels, and further define a Channel Graph

where the channel maps are presented as nodes and the independencies are represented as graph edges. AGCN [Xie, Chen and Peng \(2020b\)](#) integrates attention mechanism with GCN for analyzing the relationships between local features of points and introduces a global point graph to compensate for the relative information of individual points. PointANSL [Yan, Zheng, Li, Wang and Cui \(2020\)](#) use the general self-attention mechanism for group feature updating, and propose a adaptive sampling (AS) module to overcome the issues of FPS.

The Transformer model, which employs self-attention as a fundamental component, includes position encoding to capture the sequential order of input tokens. Position encoding is crucial to ensure that the model understands the relative positions of tokens within a sequence. Point Transformer [Zhao, Jiang, Jia, Torr and Koltun \(2021\)](#) introduce MLP-based position encoding into vector attention, and use a KNN-based downsampling module to decrease the point resolution. Follow up work, Point Transformer v2 [Wu, Lao, Jiang, Liu and Zhao \(2022a\)](#) strengthens the position encoding mechanism by applying an additional encoding multiplier to the relation vector, and designs a partition-based pooling strategy to align the geometric information.

Point Transformers are generally computationally expensive because the original self-attention module needs to generate a huge attention map. To address this problem, PatchFormer [Zhang, Wan, Shen and Wu \(2022\)](#) calculates the attention map via low-rank approximation. Similarly, FastPointTransformer [Park, Jeong, Cho and Park \(2022\)](#) introduces a lightweight local self-attention module that learns continuous positional information while reducing the space complexity. Inspired by the success of window-based Transformer in the 2D domain, Stratified Transformer [Lai, Liu, Jiang, Wang, Zhao, Liu, Qi and Jia \(2022\)](#) designs a cubic window and samples distant points as keys, but in a sparser way, to expand the receptive field. Similarly, SphereFormer [Lai, Chen, Lu, Liu and Jia \(2023\)](#) designs radial window self-attention that partitions that space into several non-overlapping narrow and long windows for exploiting long-range dependencies.

3.5. Other Representation Based

Some methods transform the original point cloud to representations other than projected images, voxels and points. Examples of such representations include *tangent images* [Tatarchenko et al. \(2018\)](#) and *lattice* [Su et al. \(2018\)](#), [Rosu et al. \(2019\)](#). In the former case, Tatarchenko et al. [Tatarchenko et al. \(2018\)](#) project local surfaces around each-point to a series of 2D tangent images and develop a tangent convolution based U-Net to extract features. In the latter case, SPLATNet [Su et al. \(2018\)](#) adapts the bilateral convolution layers (BCLs) proposed by Jampani et al. [Jampani, Kiefel and Gehler \(2016\)](#) to smoothly map disordered points onto a sparse lattice. Similarly, LatticeNet [Rosu et al. \(2019\)](#) uses a hybrid architecture that combines PointNet, which obtains low-level features, with sparse 3D

convolution, which explores global context features. These features are embedded into a sparse lattice that allows the application of standard 2D convolutions.

Although the above methods have achieved significant progress in 3D semantic segmentation, each has its own drawbacks. For instance, multi-view images have more spectral information like color/intensity but less geometric information of the scene. On the other hand, voxels have more geometric information but less spectral information. To get the best of both worlds, some methods adopt *hybrid representations* as input to learn comprehensive features of a scene. Dai et al. [Dai and Nießner \(2018\)](#) map 2D semantic features obtained by multi-view networks into 3D grids of scene. These pipelines make 3D grids attach rich 2D semantic as well as 3D geometric information so that the scene can get better segmentation by a 3D CNN. Similarly, Hung et al. [Chiang et al. \(2019\)](#) back-project 2D multi-view image features on to the 3D point cloud space and use a unified network to extract local details and global context from sub-volumes and the global scene respectively. Liu et al. [Liu et al. \(2019b\)](#) argue that voxel-based and point-based NN are computationally inefficient in high-resolution and data structuring respectively. To overcome these challenges, they propose Point-Voxel CNN (PVCNN) that represents the 3D input data as point clouds to take advantage of the sparsity to lower the memory footprint, and leverage the voxel-based convolution to obtain a contiguous memory access pattern. Jaritz et al. [Jaritz et al. \(2019\)](#) proposed MVPNet that collect 2D multi-view dense image features into 3D sparse point clouds and then use a unified network to fuse the semantic and geometric features. Also, Meyer et al. [Meyer et al. \(2019\)](#) fuse 2D image and point clouds to address 3D object detection and semantic segmentation by a unifying network. BpNet [Hu et al. \(2021\)](#) consists of 2D and 3D sub-networks with symmetric architectures, connected through a bidirectional projection module (BPM). This allows the interaction of complementary information from both visual domains at multiple architectural levels, leading to improved scene recognition by leveraging the advantages of both 2D and 3D information. The other representations based semantic segmentation methods are summarized in Table 3.

4. 3D Instance Segmentation

3D instance segmentation methods additionally distinguish between different instances of the same class. Being a more informative task for scene understanding, 3D instance segmentation is receiving increased interest from the research community. 3D instance segmentation methods are roughly divided into two directions: *proposal-based* and *proposal-free*.

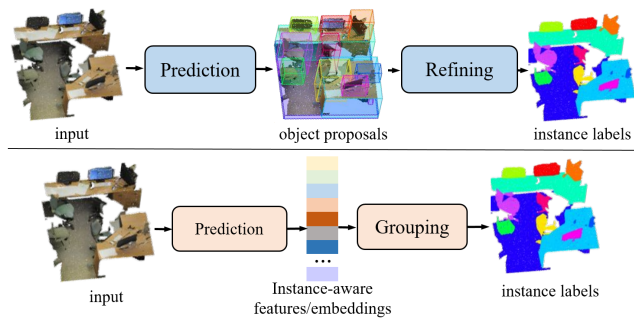
4.1. Proposal Based

Proposal-based methods first predict object proposals and then refine them to generate final instance masks (see Figure 7), breaking down the task into two main challenges. Hence, from the proposal generation point of view, these

Table 4

Summary of point based semantic segmentation methods with deep learning.

Type	Methods	Neighb. search	Feature abstraction	Coarsening	Contribution
MLP	PointNet Qi et al. (2017a)	None	MLP	None	Pioneering processing points directly
	G+RCU Engelmann et al. (2018)	None	MLP	None	Two local definition+local/global pathway
	ESC Engelmann et al. (2017)	None	MLP	None	MC/Grid Block for local defini.+RCUs for context exploit.
	HRNN Ye et al. (2018)	None	MLP	None	3P for local feature exploit.+HRNN for local context exploit.
	PointNet++ Qi et al. (2017b)	Ball/KNN	PointNet	FPS	Proposing hierarchical learning framework
	PointSIFT Jiang et al. (2018)	KNN	PointNet	FPS	PointSIFT module for local shape information
	PointWeb Zhao et al. (2019a)	KNN	PointNet	FPS	AFA for interactive feature exploitation
	Repsurf Ran et al. (2022)	KNN	PointNet	FPS	Local triangular orientation + local umbrella orientation
	PointNetXt Qian et al. (2022)	KNN	InvResMLP	FPS	Next version of PointNet
Point Convolution	RSNet Huang et al. (2018)	None	1x1 Conv	None	LDM for local context exploitation
	DPC Engelmann et al. (2020b)	DKNN	PointConv	None	Dilated KNN for expanding the receptive field
	PointWiseCNN Hua et al. (2018)	Grid	PWConv.	None	Novel point convolution
	PCCN Wang et al. (2018c)	KD index	PCCConv.	None	KD-tree index for neigh. search+novel point Conv.
	KPConv Thomas et al. (2019)	Ball	KPConv.	Grid sampling	Novel point convolution
	FlexConv Groh et al. (2018)	KD index	flexConv.	IDISS	Novel point Conv.+flex-maxpooling without subsampling
	PointCNN Li et al. (2018b)	DKNN	χ -Conv	FPS	Novel point convolution
	MCC Hermosilla et al. (2018)	Ball	MCCConv.	PDS	Novel coarsening layer+point convolution
	PointConv Wu et al. (2019b)	KNN	PointConv	FPS	Novel point convolution considering point density
	A-CNN Komarichev et al. (2019)	DKNN	ACConv	FPS	Novel neighborhood search+point convolution
	RandLA-Net Hu et al. (2020)	KNN	LocSE	RPS	LFAM with large receptive field and keeping geometric details
PolarNet Zhang et al. (2020)	None	PointNet	PolarGrid	Novel local regions definition + RingConv	
Graph Convolution	DGCNN Wang et al. (2019b)	KNN	EdgeConv	None	Novel graph convolution + updating graph
	SPG Landrieu and Simonovsky (2018)	partition	PointNet	None	Superpoint graph + parsing large-scale scene
	DeepGCNs Li et al. (2019a)	DKNN	DGConv	RPS	Adapting residual connections between layers
	SPH3D-GCN Lei et al. (2020)	Ball	SPH3D-GConv	FPS	Novel graph convolution + pooling + uppooling
	LS-GCN Wang et al. (2018a)	KNN	Spec.Conv.	FPS	Local spectral graph + Novel graph convolution
	PAN Feng et al. (2020)	Multi-direct.	LAE-Conv	PFS	Point-wise spatial attention+local graph Conv.
	TGNet Li et al. (2019b)	Ball	TGConv	PFS	Novel graph Conv.+multi-scale features explo.
	HDGCN Liang et al. (2019a)	KNN	DGConv	FPS	Depthwise graph Conv. + Pointwise Conv.
	3DCon.Net Zeng and Gevers (2018)	KNN	PointNet	Tree layer	KD tree structure
	ψ -CNN Lei et al. (2019)	Otree neig.	ψ -Conv	Tree layer	Otree structure+ Novel graph convolution
Point Transformer	PGCRNet Ma et al. (2020)	None	Conv1D	None	PointGCR to model context dependencies
	AGCN Xie et al. (2020b)	KNN	MLP	None	Point attention layer for aggregating local features
	PointANSL Yan et al. (2020)	KNN	local-nonlocal module	AS	Local-nonlocal module + adaptive sampling
	Point Transformer Zhao et al. (2021)	KNN	Point Transformer	Pooling	MLP-based relative position encoding + vector attention
	Point Transformer v2 Wu et al. (2022a)	Grid partition	PointTransformerv2	pooling	Novel position encoding + grid Pooling
	PatchFormer Zhang et al. (2022)	Boxes partition	Patch Transformer	DWConv	First linear attention + Lightweight multi-scale Transformer
	Fast Point Transformer Park et al. (2022)	Voxel partition	Fast point Transformer	Voxel-based sampl.	Lightweight local self-attention + novel position encoding
	Stratified Transformer Lai et al. (2022)	Voxel partition	Stratified Transformer	PFS	Contextual relative position encoding
	SphereFormer Lai et al. (2023)	Voxel partition	Sphereformer + cubicformer	Maxpooling	Novel spherical window for LIDAR points


Fig. 7: Illustration of two different approaches for 3D instance segmentation. **Top:** proposal-based framework. **Bottom:** proposal-free framework.

methods can be grouped into *detection-based* and *detection-free* methods.

Detection-based methods sometimes define object proposals as a 3D bounding box regression problem. 3D-SIS Hou, Dai and Nießner (2019) incorporates high-resolution

RGB images with voxels, based on the pose alignment of the 3D reconstruction, and jointly learns color and geometric features by a 3D detection backbone to predict 3D bounding box proposals. In these proposals, a 3D mask backbone predicts the final instance masks. Similarly, GPSN Yi, Zhao, Wang, Sung and Guibas (2019) introduces a 3D object proposal network termed Generative Shape Proposal Network (GPSN) that reconstructs object shapes from shape noisy observations to enforce geometric understanding. GPSN is further embedded into a 3D instance segmentation network named Region-based PointNet (R-PointNet) to reject, receive and refine proposals. Training of these networks needs to be performed step-by-step and the object proposal refinement requires expensive suppression operation. To this end, Yang et al. Yang, Wang, Clark, Hu, Wang, Markham and Trigoni (2019) introduced a novel end-to-end network named 3D-BoNet to directly learn a fixed number of 3D bounding boxes without any rejection, and then estimate an instance mask in each bounding box.

Detection-free methods include SGPW Wang, Yu, Huang and Neumann (2018d) which assumes that the points belonging to the same object instance should have very similar features. Hence, it learns a similarity matrix to predict proposals. The proposals are pruned by confidence scores of the points to generate highly credible instance proposals. However, this simple distance similarity metric learning is not informative and is unable to segment adjacent objects of the same class. To this end, 3D-MPA Engelmann, Bokeloh, Fathi, Leibe and Nießner (2020a) learns object proposals from sampled and grouped point features that vote for the same object center, and then consolidates the proposal features using a graph convolutional network enabling higher-level interactions between proposals which result in refined proposal features. AS-Net Jiang, Yan, Cai, Zheng and Xiao (2020a) uses an assignment module to assign proposal candidates and then eliminates redundant candidates by a suppression network. SoftGroup Vu, Kim, Luu, Nguyen and Yoo (2022) proposes top-down refinement to refine the instance proposal. SSTNet Liang, Li, Xu, Tan and Jia (2021) proposes an end-to-end solution of Semantic Superpoint Tree Network (SSTNet) to generate object instance proposals from scene points. A key contribution in SSTNet is an intermediate semantic superpoint tree (SST), which is constructed based on the learned semantic features of superpoints. The tree is traversed and split at intermediate nodes to generate proposals of object instances.

4.2. Proposal Free

Proposal-free methods learn feature embedding for each point and then apply clustering to obtain definitive 3D instance labels (see Figure 7) breaking down the task into two main challenges. From the embedding learning point of a view, these methods can be roughly subdivided into four categories: *2D embedding based multi-tasks learning*, *clustering based*, and *dynamic convolution based*.

2D embedding based: An example of these methods is the 3D-BEVIS Elich, Engelmann, Kontogianni and Leibe (2019) that learns 2D global instance embedding with a bird's-eye-view of the full scene. It then propagates the learned embedding onto point clouds by DGCNN Wang et al. (2019b). Another example is PanopticFusion Narita, Seno, Ishikawa and Kaji (2019) which predicts pixel-wise instance labels by 2D instance segmentation network Mask R-CNN He, Gkioxari, Dollár and Girshick (2017a) for RGB frames and integrates the learned labels into 3D volumes.

Multi-tasks learning: 3D semantic segmentation and 3D instance segmentation can influence each other. For example objects with different classes must be different instances, and objects with the same instance label must be the same class. Based on this, ASIS Wang, Liu, Shen, Shen and Jia (2019a) designs an encoder-decoder network, termed ASIS, to learn semantic-aware instance embeddings for boosting the performance of the two tasks. Similarly, JSIS3D Pham, Nguyen, Hua, Roig and Yeung (2019b) uses a unified network namely MT-PNet to predict the semantic labels of points and embedding the points into high-dimensional

feature vectors, and further propose a MV-CRF to jointly optimize object classes and instance labels. Similarly Liu et al. Liu and Furukawa (2019) and 3D-GEL Liang, Yang and Wang (2019b) adopt SSCN to generate semantic predictions and instance embeddings simultaneously, then use two GCNs to refine the instance labels. OccuSeg Han, Zheng, Xu and Fang (2020) uses a multi-task learning network to produce both occupancy signal and spatial embedding. The occupancy signal represents the number of voxel occupied by per voxel.

Clustering based: methods like MASC Liu and Furukawa (2019) rely on high performance of the SSCN Graham et al. (2018) to predict the similarity embedding between neighboring points at multiple scales and semantic topology. A simple yet effective clustering Liu, Yang, Li, Zhou, Xu, Li and Lu (2018c) is adapted to segment points into instances based on the two types of learned embeddings. MTML Lahoud, Ghanem, Pollefeys and Oswald (2019) learns two sets of feature embeddings, including the feature embedding unique to every instance and the direction embedding that orients the instance center, which provides a stronger grouping force. Similarly, PointGroup Jiang, Zhao, Shi, Liu, Fu and Jia (2020b) groups points into different clusters based on the original coordinate embedding space and the shifted coordinate embedding space. In addition, the proposed ScoreNet guides the proper cluster selection. The above methods usually group points according to point-level embeddings, without the instance-level corrections. HAIS Chen, Fang, Zhang, Liu and Wang (2021) introduce the set aggregation and intra-instance prediction to refine the instance at the object level.

Dynamic convolution based: These methods overcome the limitations of clustering based methods by generating kernels and then using them to convolve with the point features to generate instance masks. Dyco3D He, Shen and Van Den Hengel (2021) adopts the clustering algorithm to generate a kernel for convolution. Similarly, PointInst3D He, Yin, Shen and van den Hengel (2022) uses FPS to generate kernels. DKNNet Wu, Shi, Du, Lu, Cao and Zhong (2022b) introduces candidate mining and candidate aggregation to generate more instance kernels. Moreover, ISBNet Ngo, Hua and Nguyen (2023) proposes a new instance encoder combining instance-aware PFS with a point aggregation layer to generate kernels to replace clustering in DyCo3D. 3D instance segmentation methods are summarized in Table 5.

5. 3D Part Segmentation

3D part segmentation is the next finer level, after instance segmentation, where the aim is to label different parts of an instance. The pipeline of part segmentation is quite similar to that of semantic segmentation except that the labels are now for individual parts. Therefore, some existing 3D semantic segmentation networks Meng et al. (2019), Graham et al. (2018), Qi et al. (2017a), Qi et al. (2017b), Zeng and Gevers (2018), Huang et al. (2018), Thomas et al. (2019), Hua et al. (2018), Hermosilla et al. (2018), Wu

Table 5

Summary of 3D instance segmentation methods with deep learning. M←multi-view image; Me←mesh;V←voxel; P←point clouds.

Type	Methods	Input	Propo./Embed.	Prediction	Refining/Grouping	Contribution
proposal based	GSPN Yi et al. (2019)	P	GSPN		R-PointNet	New proposal generation methods
	3D-SIS Hou et al. (2019)	M+V	3D-RPN+3D-RoI		3DFCN	Learning bounding box on geometry and RGB
	3D-BoNet Yang et al. (2019)	P	Bounding box regression		Point mask prediction	Directly regressing 3D bounding box
	SGPN Wang et al. (2018d)	P	SM + SCM + PN		Non-Maximum suppression	New group proposal
	3D-MPA Engelmann et al. (2020a)	p	SSCNet		Graph ConvNet	Multi proposal aggregation strategy
	AS-Net Jiang et al. (2020a)	p	Four branches with MLPs		Candidate proposal suppression	Novel Algorithm mapping labels to candidates
	SoftGroup Vu et al. (2022)	P	Soft-grouping module		top-down refinement	Novel clustering algorithm based on dual coordinate sets
	SSTNet Liang et al. (2021)	p	Tree traversal + splitting		CliqueNet	Constructing the superpoint tree for instance segmentation
proposal free	3D-BEVIS Elich et al. (2019)	M	U-Net/FCN + 3D prop.		Mean-shift clustering	Joint 2D-3D feature
	PanopticFus Narita et al. (2019)	M	PSPNet/Mask R-CNN		FC-CRF	Coopering with semantic mapping
	ASIS Wang et al. (2019a)	P	1 encoder+ 2 decoders		ASIS module	Simultaneously performing sem./ins. segmentation tasks
	JSIS3D Pham et al. (2019b)	P	MT-PNet		MV-CRF	Simultaneously performing sem./ins. segmentation tasks
	3D-GEL Liang et al. (2019b)	P	SSCNet		GCN	Structure-aware loss function + attention-based GCN
	OccuSeg Han et al. (2020)	P	3D-U-Net		Graph-based clustering	Proposing a novel occupancy signal
	MASC Liu and Furukawa (2019)	Me	U-Net with SSConv		Clustering algorithm	Novel clustering based on affinity and mesh topology
	MTML Lahoud et al. (2019)	V	SSCNet		Mean-shift clustering	Multi-task learning
	PointGroup Jiang et al. (2020b)	P	U-Net with SSConv		Point clustering + ScoreNet	Novel clustering algorithm based on dual coordinate sets
	HAI3 Chen et al. (2021)	P	3D U-Net		Set aggregation	Hierarchical aggregation for fine-grained predictions
	Dyco3D He et al. (2021)	P	3D U-Net		Dynamic conv.	Generating kernel by clustering for convolution
	PointInst3D He et al. (2022)	P	3D U-Net		MLP	Generating kernel by FPS
	DKNet Wu et al. (2022b)	P	3D U-Net		MLP	Generating kernel by candidate mining and aggregation
	ISBNet Ngo et al. (2023)	P	3D U-Net		Box-aware dynamic conv	Generating kernel by instance aware FPS and point aggrega.

[et al. \(2019b\)](#), [Li et al. \(2018b\)](#), [Wang et al. \(2019b\)](#), [Lei et al. \(2020\)](#), [Xie et al. \(2020b\)](#), [Wang et al. \(2018c\)](#), [Groh et al. \(2018\)](#), [Lei et al. \(2019\)](#), [Su et al. \(2018\)](#), [Rosu et al. \(2019\)](#) can also be trained for part segmentation. However, these networks can not entirely tackle the difficulties of part segmentation. For example, various parts with the same semantic label might have diverse shapes, and the number of parts for an instance with the same semantic label may be different. We subdivide 3D part segmentation methods into two categories: *regular data* based and *irregular data* based as follows.

5.1. Regular Data Based

Regular data usually includes projected images [Kalogerakis, Averkiou, Maji and Chaudhuri \(2017\)](#), voxels [Wang and Lu \(2019\)](#), [Le and Duan \(2018\)](#), [Song, Chen, Li and Zhao \(2017\)](#). As for projected images, [Kalogerakis et al. \(2017\)](#) obtain a set of images from multiple views that optimally cover object surface, and then use multi-view Fully Convolutional Networks(FCNs) and surface-based Conditional Random Fields (CRFs) to predict and refine part labels separately. Voxel is a useful representation of geometric data. However, fine-grained tasks like part segmentation require high resolution voxels with more detailed structure information, which leads to high computation cost. [Wang et al. \(2019\)](#) proposed VoxSegNet to exploit more detailed information from voxels with limited resolution. They use spatial dense extraction to preserve the spatial resolution during the sub-sampling process and an attention feature aggregation (AFA) module to adaptively select scale features. [Le et al. \(2018\)](#) introduced a novel 3D CNN called PointGrid, to incorporate a constant number of points with each cell allowing the network to learn better local geometry shape

details. Furthermore, multiple model fusion can enhance the segmentation performance. Combining the advantages of images and voxels, [Song et al. \(2017\)](#) proposed a two-stream FCN, termed AppNet and GeoNet, to explore 2D appearance and 3D geometric features from 2D images. In particular, their VolNet extracts 3D geometric features from 3D volumes guiding GeoNet to extract features from a single image.

5.2. Irregular Data Based

Irregular data representations usually includes meshes [Xu et al. \(2017\)](#), [Hanocka et al. \(2019\)](#) and point clouds [Li et al. \(2018a\)](#), [Shen et al. \(2018\)](#), [Yi et al. \(2017\)](#), [Verma et al. \(2018\)](#), [Wang et al. \(2018b\)](#), [Yu et al. \(2019\)](#), [Zhao et al. \(2019b\)](#) [Yue, Wang, Tang and Chen \(2022\)](#). Mesh provides an efficient approximation to a 3D shape because it captures the flat, sharp and intricate of surface shape and topology. [Xu et al. \(2017\)](#) put the face normal and face distance histogram as the input of a two-stream framework and use the CRF to optimize the final labels. Inspired by traditional CNN, [Hanocka et al. \(2019\)](#) design novel mesh convolution and pooling to operate on the mesh edges.

As for point clouds, the graph convolution is the most commonly used pipeline. In the spectral graph domain, SyncSpecCNN [Yi et al. \(2017\)](#) introduces a Synchronized Spectral CNN to process irregular data. Specially, multi-channel convolution and parametrized dilated convolution kernels are proposed to solve multi-scale analysis and information sharing across shapes respectively. In spatial graph domain, in analogy to a convolution kernel for images, KC-Net [Shen et al. \(2018\)](#) present point-set kernel and nearest-neighbor-graph to improve PointNet with an efficient local feature exploitation structure. Similarly, [Wang et al. \(2019\)](#)

Table 6

Summary of 3D part segmentation methods. M←multi-view image; Me←mesh;V←voxel;P←point clouds; reg.←regular data; ir-reg.←irregular data.

Type	Methods	Input	Architecture	Feature extractor	Contribution
regular	ShapePCFN Kalogerakis et al. (2017)	M	Multi-stream FCN	2DConv	Per-label confidence maps + surface-based CRF
	VoxSegNet Wang and Lu (2019)	V	3DU-Net	AtrousConv	SDE for preserving the spatial resolution AFA for feature selecting
	Pointgrid Le and Duan (2018)	V	Conv-deconv	3DConv	Learning higher order local geometry shape.
	SubvolumeSup Song et al. (2017)	M+V	2-stream FCN	2D/3DConv	GeoNet/AppNet for 3/2D features exploi. + DCT for aligning.
irregular	DCN Xu, Dong and Zhong (2017)	Me	2-tream DCN & NN	DirectionalConv	DCN/NN for local feature and global feature.
	MeshCNN Hanocka, Hertz, Fish, Giryes, Fleishman and D. (2019)	Me	2D CNN	MeshConv	Novel mesh convolution and pooling
	PartNet Yu, Liu, Zhang, Zhu and Xu (2019)	P	RNN	PN	Part feature learning scheme for context and geometry feature exploitation
	SSCNN Yi, Su, Guo and Guibas (2017)	P	FCN	SpectralConv	STN for allowing weight sharing + spectral multi-scale kernel
	KCNet Shen et al. (2018)	P	PN	MLP	KNN graph on points + kernel correlation for measuring geometric affinity
	SFCN Wang, Gan, Shui, Yu, Zhang, Chen and Sun (2018b)	P	FCN	SFCConv	Novel point convolution
	SpiderCNN Xu, Fan, Xu, Zeng and Qiao (2018)	P	PN	SpiderConv	Novel point convolution
	FeaStNet Verma, Boyer and Verbeek (2018)	P	U-Net	GConv	Dynamic graph convolution filters
	Kd-Net Klokov and Lempitsky (2017)	P	Kd-tree	Affine Transformation	Using Kd-tree to build graphs and share learnable parameters
	O-CNN Wang, Liu, Guo, Sun and Tong (2017)	P	Octree	3DConv	Making 3D-CNN feasible for high-resolu. voxels
	PointCapsNet Zhao, Birdal, Deng and Tombari (2019b)	P	Encoder-decoder	PN	Semi-supervision learning
	SO-Net Li, Chen and Hee Lee (2018a)	P	Encoder-decoder	FC layers	SOM for modeling spatial distribution + un-supervision learning

[et al. \(2018b\)](#) design Shape Fully Convolutional Networks (SFCN) based on graph convolution and pooling operation, similar to FCN on images. SpiderCNN [Xu et al. \(2018\)](#) applies a special family of convolutional filters that combine simple step function with Taylor polynomial, making the filters to effectively capture intricate local geometric variations. Furthermore, FeastNet [Verma et al. \(2018\)](#) uses dynamic graph convolution operator to build relationships between filter weights and graph neighborhoods instead of relying on static graph of the above network.

A special kind of graphs, the trees (e.g. Kd-tree and Octree), work on 3D shapes with different representations and can support various CNN architectures. Kd-Net [Klokov and Lempitsky \(2017\)](#) uses a kd-tree data structure to represent point cloud connectivity. However, the networks have high computational cost. O-CNN [Wang et al. \(2017\)](#) designs an Octree data structure from 3D shapes. However, the computational cost of the O-CNN grows quadratically as the depth of tree increases.

SO-Net [Li et al. \(2018a\)](#) sets up a Self-Organization Map (SOM) from point clouds, and hierarchically learns node-wise features on this map using the PointNet architecture. However, it fails to fully exploit local features. PartNet [Yu et al. \(2019\)](#) decomposes 3D shapes in a top-down fashion, and proposes a Recursive Neural Network (RvNN) for learning the hierarchy of fine-grained parts. Zhao et al. [Zhao et al. \(2019b\)](#) introduce an encoder-decoder network, 3D-PointCapsNet, to tackle several common point cloud-related tasks. The dynamic routing scheme and the peculiar 2D latent space deployed by capsule networks, deployed in their model, bring improved performance. The 3D part segmentation methods are summarized in Table 6.

6. Applications of 3D Segmentation

We review 3D semantic segmentation methods for two main applications, unmanned systems.

6.1. Unmanned Systems

As LIDAR scanners and depth cameras become widely available and more affordable, they are increasingly being deployed in unmanned systems such as autonomous driving and mobile robots. These sensors provide realtime 3D video, generally at 30 frames per second (fps), as direct input to the system making *3D video semantic segmentation* as the primary task to understand the scene. Furthermore, in order to interact more effectively with the environment, unmanned systems generally build a *3D semantic map* of the scene. Below we review 3D video based semantic segmentation and 3D semantic map construction.

6.1.1. 3D video semantic segmentation

Compared to the 3D single frame/scan semantic segmentation methods reviewed in Section 3.1, 3D video (continuous frames/scans) semantic segmentation methods take into account the connecting spatio-temporal information between frames which is more powerful at parsing the scene robustly and continuously. Conventional convolutional neural networks (CNNs) are not designed to exploit the temporal information between frames. A common strategy is to adapt Recurrent Neural Networks or Spatio-temporal convolutional network.

Recurrent neural network based: RNNs generally work in combination with 2D CNNs to process RGB-D videos. The 2D CNN learns to extract the frame-wise spatial information and the RNN learns to extract the temporal information between the frames. Valipour et al. [Valipour, Siam, Jagersand and Ray \(2017\)](#) proposed Recurrent Fully Neural Network

to operate over a sliding window over the RGB-D video frames. Specifically, the convolutional gated recurrent unit preserves the spatial information and reduces the parameters. Similarly, Yurdakul et al. [Emre Yurdakul and Yemez \(2017\)](#) combine fully convolutional and recurrent neural network to investigate the contribution of depth and temporal information separately in the synthetic RGB-D video.

Spatio-temporal convolution based: Nearby video frames provide diverse viewpoints and additional context of objects and scenes. STD2P [He, Chiu, Keuper and Fritz \(2017b\)](#) uses a novel spatio-temporal pooling layer to aggregate region correspondences computed by optical flow and image boundary-based super-pixels. Choy et al. [Choy, Gwak and Savarese \(2019\)](#) proposed 4D Spatio-Temporary ConvNet, to directly process a 3D point cloud video. To overcome challenges in the high-dimensional 4D space (3D space and time), they introduced the 4D spatio-temporal convolution, a generalized sparse convolution, and the trilateral-stationary conditional random field that keeps spatio-temporal consistency. Similarly, based on 3D sparse convolution, Shi et al. [Shi, Lin, Wang, Hung and Wang \(2020\)](#) proposed SpSequenceNet that contains two novel modules, a cross frame-global attention module and a cross-frame local interpolation module to exploit spatial and temporal feature in 4D point clouds. PointMotionNet [Wang, Li, Sullivan, Abbott and Chen \(2022\)](#) proposes a spatio-temporal convolution that exploits a time-invariant spatial neighboring space and extracts spatio-temporal features, to distinguish the moving and static objects.

Spatio-temporal Transformer based : To capture the dynamics in point cloud video, point tracking is usually employed. However, P4Transformer [Fan, Yang and Kankanhalli \(2021\)](#) proposes a 4D convolution to embed the spatio-temporal local structures in point cloud video and further introduces a Transformer to leverage the motion information across the entire video by performing the self-attention on these embedded local features. Similarly, PST² [Wei, Liu, Xie, Ke and Guo \(2022\)](#) performs spatio-temporal self attention across adjacent frames to capture the spatio-temporal context, and proposes a resolution embedding module to enhance the resolution of feature maps by aggregating features.

6.1.2. 3D semantic map construction

Unmanned systems do not just need to avoid obstacles but also need to establish a deeper understanding of the scene such as object parsing, self localization etc. To facilitate such tasks, unmanned systems build a 3D semantic map of the scene which includes two key problems: geometric reconstruction and semantic segmentation. 3D scene reconstruction has conventionally relied on simultaneous localization and mapping system (SLAM) to obtain a 3D map without semantic information. This is followed by 2D semantic segmentation with a 2D CNN and then the 2D labels are transferred to the 3D map following an optimization (e.g. conditional random field) to obtain a 3D semantic map [Yang, Huang and Scherer \(2017\)](#). This common pipeline does not guarantee high performance of 3D semantic maps

in complex, large-scale, and dynamic scenes. Efforts have been made to enhance the robustness using association information exploitation from multiple frames, multi-model fusion and novel post-processing operations. These efforts are explained below.

Association information exploitation: mainly depends on SLAM trajectory, recurrent neural networks or scene flow. Ma et al. [Ma, Stückler, Kerl and Cremers \(2017\)](#) enforce consistency by warping CNN feature maps from multi-views into a common reference view by using the SLAM trajectory and to supervise training at multiple scales. SemanticFusion [McCormac, Handa, Davison and Leutenegger \(2017\)](#) incorporates deconvolutional neural networks with a state-of-the-art dense SLAM system, ElasticFusion, which provides long-term correspondence between frames of a video. These correspondences allow label predictions from multi-views to be probabilistically fused into a map. Similarly, using the connection information between frames provided by a recurrent unit on RGB-D videos, Xiang et al. [Xiang and Fox \(2017\)](#) proposed a data associated recurrent neural networks (DA-RNN) and integrated the output of the DA-RNN with KinectFusion, which provides a consistent semantic labeling of the 3D scene. Cheng et al. [Cheng, Sun and Meng \(2020\)](#) use a CRF-RNN-based semantic segmentation to generate the corresponding labels. Specifically, the authors proposed an optical flow-based method to deal with the dynamic factors for accurate localization. Kochanov et al. [Kochanov, Ošep, Stückler and Leibe \(2016\)](#) also use scene flow to propagate dynamic objects within the 3D semantic maps.

Multiple model fusion: Jeong et al. [Jeong, Yoon and Park \(2018\)](#) build a 3D map by estimating odometry based on GPS and IMU, and use a 2D CNN for semantic segmentation. They integrate the 3D map with semantic labels using a coordinate transformation and Bayes' update scheme. Zhao et al. [Zhao, Sun, Purkait, Duckett and Stolkin \(2018\)](#) use PixelNet and VoxelNet to exploit global context information and local shape information separately and then fuse the score maps with a softmax weighted fusion that adaptively learns the contribution of different data streams. The final dense 3D semantic maps are generated with visual odometry and recursive Bayesian update.

7. Experimental Results

Below we summarize the quantitative results of the segmentation methods discussed in Sections 3, 4 and 5 on some typical public datasets, as well as analyze these results qualitatively.

7.1. Results for 3D Semantic Segmentation

We report the results of RGB-D based semantic segmentation methods on SUN-RGB-D [Song et al. \(2015\)](#) and NYUDv2 [Silberman et al. \(2012\)](#) datasets using mAcc (mean Accuracy) and mIoU (mean Intersection over Union) as the evaluation metrics. These results of various methods are taken from the original papers and they are shown in Table 7.

Table 7

Evaluation performance regarding for RGB-D semantic segmentation methods on the SUN-RGB-D and NYUDv2. Note that the ‘%’ after the value is omitted and the symbol ‘-’ means the results are unavailable.

Methods	NYUDv2		SUN-RGB-D	
	mAcc	mIoU	mAcc	mIoU
Guo and Chen (2018)	46.3	34.8	45.7	33.7
Wang et al. (2015)	-	44.2	-	-
Mousavian et al. (2016)	52.3	39.2	-	-
Liu et al. (2018b)	50.8	39.8	50.0	39.4
Gupta et al. (2014)	35.1	28.6	-	-
Liu et al. (2018a)	51.7	41.2	-	-
Hazirbas et al. (2016)	-	-	48.3	37.3
Lin et al. (2017)	-	47.7	-	48.1
Jiang et al. (2017)	-	-	50.6	39.3
Wang and Neumann (2018)	47.3	-	-	-
Cheng et al. (2017)	60.7	45.9	58.0	-
Fan et al. (2017)	50.2	-	-	-
Li et al. (2016)	49.4	-	48.1	-
Qi et al. (2017c)	55.7	43.1	57.0	45.9
Wang et al. (2016)	60.6	38.3	50.1	33.5

We report the results of projected images/voxel/point clouds/other representation semantic segmentation methods on S3DIS Armeni et al. (2016) (both Area 5 and 6-fold cross validation), ScanNet Dai et al. (2017) (test sets), Semantic3D Hackel et al. (2017) (reduced-8 subsets) and SemanticKITTI Behley et al. (2019) (only xyz without RGB). We use mAcc, oAcc (overall accuracy) and mIoU as the evaluation metrics. These results of various methods are taken from the original papers. Table 8 reports the results.

The architectures of point cloud semantic segmentation typically focus on five main components: *basic framework*, *neighborhood search*, *features abstraction*, *coarsening*, and *pre-processing*. Below, we provide a more detailed discussion of each component.

Basic framework: Basic networks are one of the main driving forces behind the development of 3D segmentation. Generally, there are two main basic frameworks including *PointNet* and *PointNet++*. The PointNet framework utilizes shared Multi-Layer Perceptrons (MLPs) to capture point-wise features and employs max-pooling to aggregate these features into a global representation. However, it lacks the ability to learn local features due to the absence of a defined local neighborhood. Additionally, the fixed resolution of the feature map makes it challenging to adapt to deep architectures. In contrast, the PointNet++ framework introduces a novel hierarchical learning architecture. It defines local regions in a hierarchical manner and to progressively extract features from these regions. This approach enables the network to capture both local and global information, leading to improved performance. As a result, many current networks adopt the PointNet++ framework or similar variations (such as 3D U-Net). This framework significantly reduces computational and memory complexities, particularly in high-level tasks like semantic segmentation, instance segmentation, and detection.

Neighborhood search: To exploit the local features of point clouds, the neighborhood point search is introduced into networks, including the *K nearest neighbors* (KNN) Zhao

et al. (2021), Ran et al. (2022), Qian et al. (2022), Ball search Hermosilla et al. (2018), Thomas et al. (2019), Lei et al. (2020), *grid-based* search Hua et al. (2018), Wu et al. (2022a) and *tree based* search Lei et al. (2019). KNN search retrieves the *K* closest neighbors to a query point based on a distance metric, and hence lacks robustness to point clouds with varying densities. Some works integrate the *dilated mechanism* with the neighbor search to expand the receptive field Komarichev et al. (2019), Li et al. (2018b), Li et al. (2019a). Ball search involves finding all points within a specified radius (ball) around a query point. Similarly, grid-based search divides the point cloud space into a regular grid structure. Ball search and grid-based search are both useful for effectively capturing local structures and neighborhoods of varying densities.

Features abstraction: In feature abstraction, commonly used methods include *MLP-based*, *Convolution-based*, and *Transformer-based* approaches. MLP is often used to extract features from individual points in point cloud data. By passing the feature vectors of each point through multiple fully connected layers, MLP learns nonlinear point-level feature representations. MLP offers flexibility and scalability in point cloud processing. Convolution operations on point clouds typically involve aggregating (low-level) information from local points to capture local structures and contextual information. In contrast, Transformer based methods establish correlations between high-level point information through the attention mechanism, which is more helpful for high-level tasks such as point cloud segmentation.

The essence of MLP based, convolution based, and Transformer based methods is to learn the relationships between points, obtaining the robust weights. In the context of similar baseline architecture, the more comprehensive the learned point cloud relationship in the feature abstraction process, the stronger the robustness of the model becomes. Recently, MLP-based methods (e.g. Resurf Ran et al. (2022) and PointNeXt Qian et al. (2022)) exhibit better accuracy and efficiency, encouraging researchers to re-examine and further explore the potential of MLP-based approaches.

Coarsening: Coarsening, also known as downsampling or subsampling, involves reducing the number of points in the point cloud while preserving the essential structures and features. Coarsening techniques include *random sampling* Hu et al. (2020), *farthest point sampling* Qi et al. (2017a,b), *tree-based* methods Lei et al. (2019) and mesh-based decimation Lei, Akhtar, Shah and Mian (2023). This step helps to reduce computational complexity and improve efficiency in subsequent stages of the segmentation process. Random sampling is simple and computationally efficient but may not select the most optimal points in maintaining local and global structure. This can potentially lead to information loss in feature rich regions. Farthest point sampling is widely used in networks as it ensures a more even spatial distribution of the selected points and can help preserve global structures. However, local structures can still get destroyed with farthest point sampling. Tree-based methods leverage hierarchical tree structures, such as an octree, to partition the point cloud

Table 8

Evaluation performance regarding for projected images, voxel, point clouds and other representation semantic segmentation methods on the S3DIS, ScanNet, Semantic3D and SemanticKITTI. Note: the ‘%’ after the value is omitted, the symbol ‘–’ means the results are unavailable, the dotted line means the subdivision of methods according to the type of architecture.

Method	Type	S3DIS		6-fold mIoU	ScanNet test set		Semantic3D reduced-8		SemanticKITTI only xyz	
		mAcc	mIoU		oAcc	mIoU	oAcc	mIoU	mAcc	mIoU
Lawin et al. Lawin et al. (2017)	projection	–	–	–	–	–	88.9	58.5	–	–
Boulch et al. Boulch et al. (2017)		–	–	–	–	–	91.0	67.4	–	–
Wu et al. Wu et al. (2018a)		–	–	–	–	–	–	–	–	37.2
Wang et al. Wang et al. (2018e)		–	–	–	–	–	–	–	–	39.8
Wu et al. Wu et al. (2019a)		–	–	–	–	–	–	–	–	44.9
Milioto et al. Milioto et al. (2019)		–	–	–	–	–	–	–	–	52.2
Xu et al. Xu et al. (2020)		–	–	–	–	–	–	–	–	55.9
RangViT Ando et al. (2023)		–	–	–	–	–	–	–	–	55.9
RangFormer Kong et al. (2023)		–	–	–	–	–	–	–	–	64.0
Tchapmi et al. Tchapmi et al. (2017)		voxel	57.35	48.92	48.92	–	–	88.1	61.30	–
Meng et al. Meng et al. (2019)	–		78.22	–	–	–	–	–	–	–
Liu et al. Liu et al. (2017)	–	70.76	–	–	–	–	–	–	–	
PointNet Qi et al. (2017a)	point	48.98	41.09	47.71	–	14.69	–	–	29.9	17.9
G+RCU Engelmann et al. (2018)		59.10	52.17	58.27	75.53	–	–	–	57.59	29.9
ESC Engelmann et al. (2017)		54.06	45.14	49.7	63.4	–	–	–	40.9	26.4
HRNN Ye et al. (2018)		71.3	53.4	–	76.5	–	–	–	49.2	34.5
PointNet++ Qi et al. (2017b)		–	50.04	54.4	71.40	34.26	–	–	–	–
PointWeb Zhao et al. (2019a)		66.64	60.28	66.7	85.9	–	–	–	–	–
PointSIFT Jiang et al. (2018)		–	70.23	70.2	–	41.5	–	–	–	–
Resurf Ran et al. (2022)		76.0	68.9	74.3	–	70.0	–	–	–	–
PointNeXt Qian et al. (2022)		–	70.5	74.9	–	71.2	–	–	–	–
RSNet Huang et al. (2018)		59.42	56.5	56.47	–	39.35	–	–	–	–
DPC Engelmann et al. (2020b)		68.38	61.28	–	–	59.2	–	–	–	–
PointwiseCNN Hua et al. (2018)		56.5	–	–	–	–	–	–	–	–
PCCN Wang et al. (2018c)		67.01	58.27	–	–	49.8	–	–	–	–
PointCNN Li et al. (2018b)		63.86	57.26	65.3	85.1	45.8	–	–	–	–
KPCConv Thomas et al. (2019)		–	67.1	70.6	–	66.6	92.9	74.6	–	–
PointConv Wu et al. (2019b)		–	50.34	–	–	55.6	–	–	–	–
A-CNN Komarichev et al. (2019)		–	–	–	85.4	–	–	–	–	–
RandLA-Net Hu et al. (2020)		–	–	70.0	–	–	94.8	77.4	–	53.9
PolarNet Zhang et al. (2020)		–	–	–	–	–	–	–	–	54.3
DGCNN Wang et al. (2019b)		–	56.1	56.1	–	–	–	–	–	–
SPG Landrieu and Simonovsky (2018)		66.50	58.04	62.1	–	–	94.0	73.2	–	–
SPH3D-GCN Lei et al. (2020)		65.9	59.5	68.9	–	61.0	–	–	–	–
DeepGCNs Li et al. (2019a)		–	60.0	–	–	–	–	–	–	–
PointGCRNet Ma et al. (2020)		–	52.43	–	–	60.8	–	–	–	–
AGCN Xie et al. (2020b)		–	–	56.63	–	–	–	–	–	–
PAN Feng et al. (2020)		–	66.3	–	86.7	42.1	–	–	–	–
TGNet Li et al. (2019b)		–	58.7	–	66.2	–	–	–	–	–
HDGCN Liang et al. (2019a)		65.81	59.33	66.85	–	–	–	–	–	–
3DContextNet Zeng and Gevers (2018)		74.5	55.6	55.6	–	–	–	–	–	–
PGCRNet Ma et al. (2020)		–	54.4	–	–	–	–	69.5	–	–
AGCN Xie et al. (2020b)	74.5	55.6	55.6	–	–	–	–	–	–	
PointANSL Yan et al. (2020)	–	62.6	68.7	–	–	66.6	–	–	–	
Point Transformer Zhao et al. (2021)	76.5	70.4	73.5	–	–	–	–	–	–	
Point Transformer v2 Wu et al. (2022a)	77.9	71.6	–	–	75.2	–	–	–	–	
PatchFormer Zhang et al. (2022)	–	68.1	–	–	–	–	–	–	–	
Fast Point Transformer Park et al. (2022)	77.3	70.1	–	–	–	–	–	–	–	
Stratify Transformer Lai et al. (2022)	78.1	72.0	–	–	73.7	–	–	–	–	
SphereFormer Lai et al. (2023)	–	–	–	–	–	–	–	–	78.4	
TangentConv Tatarchenko et al. (2018)	others	62.2	52.8	–	80.1	40.9	89.3	66.4	–	–
SPLATNet Su et al. (2018)		–	–	–	–	39.3	–	–	–	–
LatticeNet Rosu et al. (2019)		–	–	–	–	64.0	–	–	–	52.9
Hung et al. Chiang et al. (2019)		–	–	–	–	63.4	–	–	–	–
PVCNN Liu et al. (2019b)		87.12	58.98	–	–	–	–	–	–	–
MVPNet Jaritz et al. (2019)		–	–	–	–	66.4	–	–	–	–
BPNet Hu et al. (2021)		–	–	–	–	74.9	–	–	–	–

and perform coarsening. Mesh based methods must convert the point cloud to a mesh first before it can decimate it. This adds a computational overhead to the already expensive mesh decimation process. Moreover, creating a mesh from complex and sparse point clouds obtained from LiDAR sensors is not always possible [Lei et al. \(2023\)](#).

The above methods are hand-crafted or engineered techniques that do not involve learning parameters directly from the data, which determines the sub-sampling pattern based on predefined rules or heuristics, without explicitly optimizing for the task at hand. Therefore, some works propose *learnable coarsening methods* that integrate a learnable layer into the coarsening module such as pooling [Groh et al.](#)

Table 9

Evaluation performance regarding for 3D instance segmentation methods on the ScanNet. Note: the ‘%’ after the value is omitted.

Methods	mAP	bath.	bed	book.	cabi.	chair	count.	curt.	desk	door	other	pict.	refr.	shower.	sink	sofa	table	toilet	wind.
GSPN Yi et al. (2019)	30.6	50.0	40.5	31.1	34.8	58.9	5.4	6.8	12.6	28.3	29.0	2.8	21.9	21.4	33.1	39.6	27.5	82.1	24.5
3D-SIS Hou et al. (2019)	38.2	100	43.2	24.5	19.0	57.7	1.3	26.3	3.3	32.0	24.0	7.5	42.2	85.7	11.7	69.9	27.1	88.3	23.5
3D-BoNet Yang et al. (2019)	48.8	100	67.2	59.0	30.1	48.4	9.8	62.0	30.6	34.1	25.9	12.5	43.4	79.6	40.2	49.9	51.3	90.9	43.9
SGPN Wang et al. (2018d)	14.3	20.8	39.0	16.9	6.5	27.5	2.9	6.9	0	8.7	4.3	1.4	2.7	0	11.2	35.1	16.8	43.8	13.8
3D-MPA Engelmann et al. (2020a)	61.1	100	83.3	76.5	52.6	75.6	13.6	58.8	47.0	43.8	43.2	35.8	65.0	85.7	42.9	76.5	55.7	100	43.0
SoftGroup Vu et al. (2022)	76.1	100	80.8	84.5	71.6	86.2	24.3	82.4	65.5	62.0	73.4	69.9	79.1	98.1	71.6	84.4	76.9	100	59.4
SSTNet Liang et al. (2021)	69.8	100	69.7	88.8	55.6	80.3	38.7	62.6	41.7	55.6	58.5	70.2	60.0	100	82.4	72.0	69.2	100	50.9
3D-BEVIS Elich et al. (2019)	24.8	66.7	56.6	7.6	3.5	39.4	2.7	3.5	9.8	9.8	3.0	2.5	9.8	37.5	12.6	60.4	18.1	85.4	17.1
PanopticFus. Narita et al. (2019)	47.8	66.7	71.2	59.5	25.9	55.0	0	61.3	17.5	25.0	43.4	43.7	41.1	85.7	48.5	59.1	26.7	94.4	35.9
OccuSeg Han et al. (2020)	67.2	100	75.8	68.2	57.6	84.2	47.7	50.4	52.4	56.7	58.5	45.1	55.7	100	75.1	79.7	56.3	100	46.7
MTML Lahoud et al. (2019)	54.9	100	80.7	58.8	32.7	64.7	0.4	81.5	18.0	41.8	36.4	18.2	44.5	100	44.2	68.8	57.1	100	39.6
PointGroup Jiang et al. (2020b)	63.6	100	76.5	62.4	50.5	79.7	11.6	69.6	38.4	44.1	55.9	47.6	59.6	100	66.6	75.6	55.6	99.7	51.3
HAIS Chen et al. (2021)	69.9	100	84.9	82.0	67.5	80.8	27.9	75.7	46.5	51.7	59.6	55.9	60.0	100	65.4	76.7	67.6	99.4	56.0
Dyco3D He et al. (2021)	64.1	100	84.1	89.3	53.1	80.2	11.5	58.8	44.8	43.8	53.7	43.0	55.0	85.7	53.4	76.4	65.7	98.7	56.8
DKNet Wu et al. (2022b)	71.8	100	81.4	78.2	61.9	87.2	22.4	75.1	56.9	67.7	58.5	72.4	63.3	98.1	51.5	81.9	73.6	100	61.7
ISBNet Ngo et al. (2023)	76.3	100	87.3	71.7	66.6	85.8	50.8	66.7	76.4	64.3	67.6	68.8	82.5	100	77.3	74.1	77.7	100	55.6

(2018), Lai et al. (2023), Wu et al. (2022a), Zhao et al. (2021), attention mechanism Yan et al. (2020).

Pre-processing: Pre-processing is an essential step in point cloud semantic segmentation that involves preparing and transforming the raw point cloud data before feeding it into the segmentation network. Pre-processing aims to enhance the quality, consistency, and suitability of the data for the segmentation task. Some common aspects of pre-processing in point cloud segmentation include *data normalization*, *data augmentation*, *outlier removal*, and *point registration*.

Point clouds often have varying scales, which can negatively affect the performance of segmentation networks. Data normalization involves scaling the point cloud data to a standard range or unit sphere to ensure consistent scales across different point. For example, the number of ShapNet object point is generally fixed as 4096. For the complexity scene, early works Xu, Ding, Zhao and Qi (2021), Qi et al. (2017a) divided raw point clouds into smaller ones (e.g. 4096 points, 1m³ blocks) so that the processing does not require large memory. However, this strategy might break down the semantic continuity of the scene. Recent works Qian et al. (2022), Lai et al. (2023), Wu et al. (2022a), Zhao et al. (2021), Lei et al. (2023) input the complete scene into the network, but that requires more computational sources. Moreover, these works tend to down sample the point cloud in the pre-processing stage.

7.2. Results for 3D Instance Segmentation

We report the results of 3D instance segmentation methods on ScanNet Dai et al. (2017) datasets, and choose mAP as the evaluation metrics. These results of these methods are taken from the ScanNet Benchmark Challenge website, and they are shown in Table 9 and summarized in Figure 8. The table and figure shows that:

ISBNet Ngo et al. (2023) has the state-of-the-art performance, with 76.3% average precision on ScanNet dataset at the time of this view. It also achieves the best instance segmentation performance on most classes, including ‘bathtub’, ‘counter’, ‘shower curtain’, ‘table’, ‘toilet’ and so on.

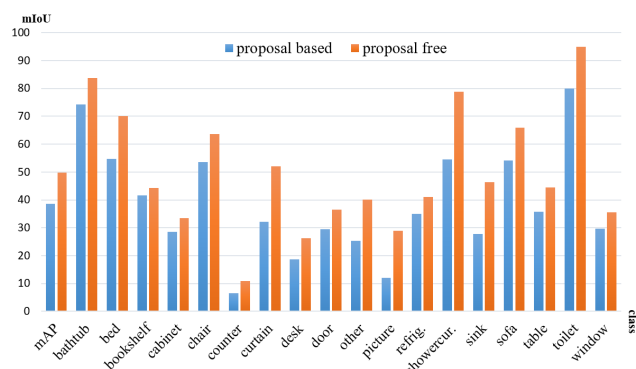


Fig. 8: Evaluation performance regarding for 3D instance segmentation architecture, including proposal based and proposal free, on the different class of ScanNet. For simplicity, we omit the ‘%’ after the value.

Most methods have better segmentation performance on large scale classes such as ‘bathtub’ and ‘toilet’, and have poor segmentation performance on small scale classes such as ‘counter’, ‘desk’ and ‘picture’. Therefore, the instance segmentation of small objects is a prominent challenge.

In proposal-based methods, specifically the 2D embedding propagating-based methods such as 3D-BEVIS Elich et al. (2019) and PanoticFusion Narita et al. (2019), they tend to exhibit poorer performance compared to other proposal-free methods. This is primarily because simple embedding propagation techniques are more susceptible to error labels, leading to inaccuracies in the instance segmentation results.

Proposal-free methods demonstrate superior performance compared to proposal-based methods in instance segmentation across all classes, particularly for small objects like ‘curtain’, ‘picture’, ‘shower curtain’, and ‘sink.’ Unlike proposal-based methods that rely on the accuracy of proposal generation, proposal-free methods circumvent this issue entirely. They directly consider the entire point cloud and its global features, enabling more precise and comprehensive instance segmentation. By avoiding the need for proposal generation,

Table 10

Evaluation performance regarding for 3D part segmentation on the ShapeNet. Note: the '%' after the value is omitted, the symbol '-' means the results are unavailable.

Methods	Ins. mIoU	Methods	Ins. mIoU
VV-Net Meng et al. (2019)	87.4	LatticeNet Su et al. (2018)	83.9
SSCNet Graham et al. (2018)	86.0	SGPN Wang et al. (2018d)	85.8
PointNet Qi et al. (2017a)	83.7	ShapePFCN Kalogerakis et al. (2017)	88.4
PointNet++ Qi et al. (2017b)	85.1	VoxSegNet Wang and Lu (2019)	87.5
3DContextNet Zeng and Gevers (2018)	84.3	Pointgrid Le and Duan (2018)	86.4
RSNet Huang et al. (2018)	84.9	KPCConv Thomas et al. (2019)	86.4
MCC Hermosilla et al. (2018)	85.9	SO-Net Li et al. (2018a)	84.9
PointConv Wu et al. (2019b)	85.7	PartNet Yu et al. (2019)	87.4
DGCNN Wang et al. (2019b)	85.1	SyncSpecCNN Yi et al. (2017)	84.7
SPH3D-GCN Lei et al. (2020)	86.8	KCNet Yi et al. (2017)	84.7
AGCN Xie et al. (2020b)	85.4	PointCNN Li et al. (2018b)	86.1
PCCN Wang et al. (2018c)	85.9	SpiderCNN Xu et al. (2018)	85.3
Flex-Conv Groh et al. (2018)	85.0	FeaStNet Verma et al. (2018)	81.5
ψ -CNN Lei et al. (2019)	86.8	Kd-Net Klokov and Lempitsky (2017)	82.3
SPLATNet Su et al. (2018)	84.6	O-CNN Wang et al. (2017)	85.9
DRGCNN Yue et al. (2022)	86.2		

proposal-free methods can achieve better results by taking into account the overall context and characteristics of the point cloud.

7.3. Results for 3D Part Segmentation

We report the results of 3D part segmentation methods on ShapeNet [Yi et al. \(2016\)](#) datasets and use Ins. mIoU as the evaluation metric. These results of various methods are taken from the original papers and they are shown in Table 10. We can find that part segmentation performance of all methods is quite similar. one underlying assumption is that objects in ShapeNet datasets are synthetic, normalized in scale, aligned in pose, and lack scene context. This makes part segmentation network difficult to extract rich context features. Another underlying assumption is that the point clouds in synthetic scene without background noise is more simpler and cleaner than ones in real scene, so that the geometric features of point clouds is easy to exploitation. The accuracy performance of various part segmentation network is difficult to be effectively distinguished.

8. Discussion and Conclusion

3D segmentation using deep learning techniques has made significant progress during recent years. However, this is just the beginning and significant developments lie ahead of us. Below, we present some outstanding issues and identify potential research directions.

- *Synthetic datasets with richer information for multiple tasks:* Synthetic datasets gradually play an important role on semantic segmentation due to the low cost and diverse scenes that can be generated [Brodeur et al. \(2017\)](#), [Wu et al. \(2018b\)](#) compared to real datasets [Dai et al. \(2017\)](#), [Armeni et al. \(2016\)](#), [Hackel et al. \(2017\)](#). It is well known that the information contained in training data determine the upper limit of the scene parsing accuracy. Existing datasets lack important semantic information, such as material, and texture information, which is more crucial for segmentation with similar color or geometric information. Besides,

most exiting datasets are generally designed for a single task. Currently, only a few semantic segmentation datasets also contain labels for instances [Dai et al. \(2017\)](#) and scene layout [Song et al. \(2015\)](#) to meet the multi-task objective.

- *Unified network for multiple tasks:* It is expensive and impractical for a system to accomplish different computer vision tasks by various deep learning networks. Towards fundamental feature exploitation of scene, Semantic segmentation has strong consistency with some tasks, such as depth estimation [Meyer et al. \(2019\)](#), [Liu et al. \(2015\)](#), [Guo and Chen \(2018\)](#), [Liu et al. \(2018b\)](#), scene completion [Dai et al. \(2018\)](#), [Xia, Liu, Li, Zhu, Ma, Li, Hou and Qiao \(2023\)](#), [Zhang, Han, Dong, Li, Yin and Yang \(2023\)](#), instance segmentation [Liang et al. \(2019b\)](#), [Pham et al. \(2019b\)](#), [Han et al. \(2020\)](#), and object detection [Meyer et al. \(2019\)](#), [Lian, Li and Chen \(2022\)](#). These tasks could cooperate with each other to improve performance in a unified network because they exhibit certain correlations and shared feature representations.
- *Multiple modals for segmentation:* Semantic segmentation using multiple representations, such as projected images, voxels, and point clouds, has the potential to achieve higher accuracy. Single representation limits segmentation accuracy due to the limited scene information in some practical scenarios. For instance, LiDAR measurements become sparser as the distance increases, and incorporating high-resolution image data can improve performance on distant objects. Therefore, utilizing multiple representations, also known as multiple modalities, can be an alternative way to enhance segmentation performance [Dai and Nießner \(2018\)](#), [Chiang et al. \(2019\)](#), [Liu et al. \(2019b\)](#), [Hu et al. \(2021\)](#). Moreover, segmenting point cloud with large image models (such as SAM [Kirillov, Mintun, Ravi, Mao, Rolland, Gustafson, Xiao, Whitehead, Berg, Lo et al. \(2023\)](#)) and natural language models like ChatGPT can be popular approaches. The

advanced capabilities of large models enable them to capture intricate patterns and semantic relationships, leading to improved performance and accuracy in segmentation tasks.

- *Interpretable and sparse feature abstraction:* Various features abstraction, including MLP, Convolution and Transformer, have undergone significant development. Feature abstraction modules may prioritize generating interpretable feature representations, enabling them to provide explanations for model decisions, visualizations of points of interest, and other interpretability functions. Moreover, in scenarios involving large-scale data and limited resources, the feature abstraction module improve computational efficiency.
- *Weakly-supervised and unsupervised segmentation:* Deep learning has gained significant success in 3D segmentation, but heavily hinges on large-scale labelled training samples. Weakly-supervised learning refers to a training approach where the model is trained with limited or incomplete supervision. Unsupervised learning only use unlabelled training samples. weakly-supervised [Su, Xu and Jia \(2023\)](#), [Shi, Wei, Li, Liu and Lin \(2022\)](#) and unsupervised [Xiao, Huang, Guan, Zhang, Lu and Shao \(2023\)](#) paradigms are considered as an alternative to relax the impractical requirement of large-scale labelled datasets.
- *Real-time and incremental segmentation:* Real-time 3D scene parsing is crucial for some applications such as autonomous driving and mobile robots. However, most existing 3D semantic segmentation methods mainly focus on the improvement of segmentation accuracy but rarely focus on real-time performance. A few lightweight 3D semantic segmentation networks realize real-time by pre-processing point clouds into other presentations such as projected images [Wu et al. \(2018a\)](#), [Wu et al. \(2019a\)](#), [Park, Kim, Kim and Jo \(2023\)](#), [Ando et al. \(2023\)](#). Additionally, incremental segmentation will become an important research direction, allowing models to incrementally update and adapt in dynamic scenes.
- *3D video semantic segmentation:* Like 2D video semantic segmentation, A handful of works try to exploit 4D spatio-temporal features on 3D videos (also call 4D point clouds) [Wei et al. \(2022\)](#), [Fan et al. \(2021\)](#). From these works, it can be seen that the spatio-temporal features can help improve the robustness of 3D video or dynamic 3D scene semantic segmentation.

We provided a comprehensive survey of the recent development in 3D segmentation using deep learning techniques, including 3D semantic segmentation, 3D instance segmentation and 3D part segmentation. We presented a comprehensive performance comparison and merit of various methods

in each category, with potential research directions being listed.

References

- Ando, A., Gidaris, S., Bursuc, A., Puy, G., Boulch, A., Marlet, R., 2023. Rangevit: Towards vision transformers for 3d semantic segmentation in autonomous driving, in: Proceedings of the IEEE/CVF Conference on Computer Vision and Pattern Recognition, pp. 5240–5250.
- Armeni, I., Sener, O., Zamir, A., Jiang, H., Brilakis, I., Fischer, M., Savarese, S., 2016. 3d semantic parsing of large-scale indoor spaces, in: Proceedings of the IEEE/CVF Conference on Computer Vision and Pattern Recognition, pp. 1534–1543.
- Behley, J., Garbade, M., Milioto, A., Quenzel, J., Behnke, S., Stachniss, C., Gall, J., 2019. Semantickitti: A dataset for semantic scene understanding of lidar sequences, in: Proceedings of the IEEE/CVF International Conference on Computer Vision, IEEE. pp. 9297–9307.
- Bello, S., Yu, S., Wang, C., Adam, J., Li, J., 2020. deep learning on 3d point clouds. Remote Sensing 12, 1729.
- Boulch, A., Guerry, J., Le Saux, B., Audebert, N., 2018. Snapnet: 3d point cloud semantic labeling with 2d deep segmentation networks. Computers & Graphics 71, 189–198.
- Boulch, A., Le Saux, B., Audebert, N., 2017. Unstructured point cloud semantic labeling using deep segmentation networks. 3dor@ eurographics 2, 7.
- Brodeur, S., Perez, E., Anand, A., Golemo, F., Celotti, L., Strub, F., Rouat, J., Larochelle, H., Courville, A., 2017. Home: A household multimodal environment. arXiv preprint arXiv:1711.11017 .
- Cao, Y., Shen, C., Shen, H., 2016. Exploiting depth from single monocular images for object detection and semantic segmentation. IEEE Transactions on Image Processing 26, 836–846.
- Chang, A., Dai, A., Funkhouser, T., Halber, M., Niebner, M., Savva, M., Song, S., Zeng, A., Zhang, Y., 2017. Matterport3d: Learning from rgb-d data in indoor environments, in: 2017 International Conference on 3D Vision (3DV), IEEE. pp. 667–676.
- Chen, S., Fang, J., Zhang, Q., Liu, W., Wang, X., 2021. Hierarchical aggregation for 3d instance segmentation, in: Proceedings of the IEEE/CVF International Conference on Computer Vision, pp. 15467–15476.
- Chen, X., Golovinskiy, A., Funkhouser, T., 2009. A benchmark for 3d mesh segmentation. ACM Transactions on Graphics 28, 1–12.
- Cheng, J., Sun, Y., Meng, M.Q.H., 2020. Robust semantic mapping in challenging environments. Robotica 38, 256–270.
- Cheng, Y., Cai, R., Li, Z., Zhao, X., Huang, K., 2017. Locality-sensitive deconvolution networks with gated fusion for rgb-d indoor semantic segmentation, in: Proceedings of the IEEE/CVF Conference on Computer Vision and Pattern Recognition, pp. 3029–3037.
- Chiang, H.Y., Lin, Y.L., Liu, Y.C., Hsu, W.H., 2019. A unified point-based framework for 3d segmentation, in: Processing of the International Conference on 3D Vision, IEEE. pp. 155–163.
- Chollet, F., 2017. Xception: Deep learning with depthwise separable convolutions, in: Proceedings of the IEEE/CVF Conference on Computer Vision and Pattern Recognition, pp. 1251–1258.
- Choy, C., Gwak, J., Savarese, S., 2019. 4d spatio-temporal convnets: Minkowski convolutional neural networks, in: Proceedings of the IEEE/CVF Conference on Computer Vision and Pattern Recognition, pp. 3075–3084.
- Coupric, C., Farabet, C., Najman, L., LeCun, Y., 2013. Indoor semantic segmentation using depth information. arXiv preprint arXiv:1301.3572 .
- Dai, A., Chang, A., Savva, M., Halber, M., Funkhouser, T., Nießner, M., 2017. Scannet: Richly-annotated 3d reconstructions of indoor scenes, in: Proceedings of the IEEE/CVF Conference on Computer Vision and Pattern Recognition, pp. 5828–5839.
- Dai, A., Nießner, M., 2018. 3dmv: Joint 3d-multi-view prediction for 3d semantic scene segmentation, in: Proceedings of the European Conference on Computer Vision, pp. 452–468.

- Dai, A., Ritchie, D., Bokeloh, M., Reed, S., Sturm, J., Nießner, M., 2018. Scancomplete: Large-scale scene completion and semantic segmentation for 3d scans, in: Proceedings of the IEEE/CVF Conference on Computer Vision and Pattern Recognition, pp. 4578–4587.
- Elich, C., Engelmann, F., Kontogianni, T., Leibe, B., 2019. 3d bird's-eye-view instance segmentation, in: German Conference on Pattern Recognition, Springer. pp. 48–61.
- Emre Yurdakul, E., Yemez, Y., 2017. Semantic segmentation of rgb-d videos with recurrent fully convolutional neural networks, in: Proceedings of the IEEE/CVF International Conference on Computer Vision Workshops, pp. 367–374.
- Engelmann, F., Bokeloh, M., Fathi, A., Leibe, B., Nießner, M., 2020a. 3dmpa: Multi-proposal aggregation for 3d semantic instance segmentation, in: Proceedings of the IEEE/CVF Conference on Computer Vision and Pattern Recognition, pp. 9031–9040.
- Engelmann, F., Kontogianni, T., Hermans, A., Leibe, B., 2017. Exploring spatial context for 3d semantic segmentation of point clouds, in: Proceedings of the IEEE/CVF International Conference on Computer Vision Workshops, pp. 716–724.
- Engelmann, F., Kontogianni, T., Leibe, B., 2020b. Dilated point convolutions: On the receptive field size of point convolutions on 3d point clouds, in: 2020 IEEE International Conference on Robotics and Automation (ICRA), IEEE. pp. 9463–9469.
- Engelmann, F., Kontogianni, T., Schult, J., Leibe, B., 2018. Know what your neighbors do: 3d semantic segmentation of point clouds, in: Proceedings of the European Conference on Computer Vision, pp. 0–0.
- Fan, H., Mei, X., Prokhorov, D., Ling, H., 2017. Rgb-d scene labeling with multimodal recurrent neural networks, in: Proceedings of the IEEE/CVF Conference on Computer Vision and Pattern Recognition Workshops, pp. 9–17.
- Fan, H., Yang, Y., Kankanhalli, M., 2021. Point 4d transformer networks for spatio-temporal modeling in point cloud videos, in: Proceedings of the IEEE/CVF conference on computer vision and pattern recognition, pp. 14204–14213.
- Feng, M., Zhang, L., Lin, X., Gilani, S.Z., Mian, A., 2020. Point attention network for semantic segmentation of 3d point clouds. *Pattern Recognition*, 107446.
- Fooladgar, F., Kasaei, S., 2020. A survey on indoor rgb-d semantic segmentation: from hand-crafted features to deep convolutional neural networks. *Multimedia Tools and Applications* 79, 4499–4524.
- Geiger, A., Lenz, P., Urtasun, R., 2012. Are we ready for autonomous driving? the kitti vision benchmark suite, in: Proceedings of the IEEE/CVF Conference on Computer Vision and Pattern Recognition, IEEE. pp. 3354–3361.
- Graham, B., Engelcke, M., Van Der Maaten, L., 2018. 3d semantic segmentation with submanifold sparse convolutional networks, in: Proceedings of the IEEE/CVF Conference on Computer Vision and Pattern Recognition, pp. 9224–9232.
- Groh, F., Wieschollek, P., Lensch, H.P., 2018. Flex-convolution, in: Asian Conference on Computer Vision, Springer. pp. 105–122.
- Guerry, J., Bouch, A., Le Saux, B., Moras, J., Plyer, A., Filliat, D., 2017. Snapnet-r: Consistent 3d multi-view semantic labeling for robotics, in: Proceedings of the IEEE/CVF International Conference on Computer Vision Workshops, pp. 669–678.
- Guo, Y., Chen, T., 2018. Semantic segmentation of rgb-d images based on deep depth regression. *Pattern Recognit. Lett.* 109, 55–64.
- Guo, Y., Wang, H., Hu, Q., Liu, H., Liu, L., Bennamoun, M., 2020. Deep learning for 3d point clouds: A survey. *IEEE Transactions on Pattern Analysis and Machine Intelligence*.
- Gupta, S., Girshick, R., Arbeláez, P., Malik, J., 2014. Learning rich features from rgb-d images for object detection and segmentation, in: Computer Vision—ECCV 2014: 13th European Conference, Zurich, Switzerland, September 6–12, 2014, Proceedings, Part VII 13, Springer. pp. 345–360.
- Hackel, T., Savinov, N., Ladicky, L., Wegner, J., Schindler, K., Pollefeys, M., 2017. Semantic3d.net: A new large-scale point cloud classification benchmark. *arXiv preprint arXiv:1704.03847*.
- Han, L., Zheng, T., Xu, L., Fang, L., 2020. Occuseg: Occupancy-aware 3d instance segmentation, in: Proceedings of the IEEE/CVF Conference on Computer Vision and Pattern Recognition, pp. 2940–2949.
- Hanocka, R., Hertz, A., Fish, N., Giryas, R., Fleishman, S., D., C.O., 2019. Meshcnn: a network with an edge. *ACM Transactions on Graphics* 38, 1–12.
- Hazirbas, C., Ma, L., Domokos, C., Cremers, D., 2016. Fusetnet: Incorporating depth into semantic segmentation via fusion-based cnn architecture, in: Proc. Asian Conf. Compu. Vis., Springer. pp. 213–228.
- He, K., Gkioxari, G., Dollár, P., Girshick, R., 2017a. Mask r-cnn, in: Proceedings of the IEEE/CVF International Conference on Computer Vision, pp. 2961–2969.
- He, T., Shen, C., Van Den Hengel, A., 2021. Dyco3d: Robust instance segmentation of 3d point clouds through dynamic convolution, in: Proceedings of the IEEE/CVF conference on computer vision and pattern recognition, pp. 354–363.
- He, T., Yin, W., Shen, C., van den Hengel, A., 2022. Pointinst3d: Segmenting 3d instances by points, in: Proceedings of the European Conference on Computer Vision, Springer. pp. 286–302.
- He, Y., Chiu, W.C., Keuper, M., Fritz, M., 2017b. Std2p: Rgb-d semantic segmentation using spatio-temporal data-driven pooling, in: Proceedings of the IEEE/CVF Conference on Computer Vision and Pattern Recognition, pp. 4837–4846.
- Hermosilla, P., Ritschel, T., Vázquez, P.P., Vinacua, À., Ropinski, T., 2018. Monte carlo convolution for learning on non-uniformly sampled point clouds. *ACM Transactions on Graphics* 37, 1–12.
- Höft, N., Schulz, H., Behnke, S., 2014. Fast semantic segmentation of rgb-d scenes with gpu-accelerated deep neural networks, in: Joint German/Austrian Conference on Artificial Intelligence, Springer. pp. 80–85.
- Hou, J., Dai, A., Nießner, M., 2019. 3d-sis: 3d semantic instance segmentation of rgb-d scans, in: Proceedings of the IEEE/CVF Conference on Computer Vision and Pattern Recognition, pp. 4421–4430.
- Hu, Q., Yang, B., Xie, L., Rosa, S., Guo, Y., Wang, Z., Trigoni, N., Markham, A., 2020. Randla-net: Efficient semantic segmentation of large-scale point clouds, in: Proceedings of the IEEE/CVF Conference on Computer Vision and Pattern Recognition, pp. 11108–11117.
- Hu, W., Zhao, H., Jiang, L., Jia, J., Wong, T.T., 2021. Bidirectional projection network for cross dimension scene understanding, in: Proceedings of the IEEE/CVF Conference on Computer Vision and Pattern Recognition, pp. 14373–14382.
- Hua, B., Pham, Q., Nguyen, D., Tran, M., Yu, L., Yeung, S., 2016. Scenenn: A scene meshes dataset with annotations, in: Processing of the International Conference on 3D Vision, IEEE. pp. 92–101.
- Hua, B.S., Tran, M.K., Yeung, S.K., 2018. Pointwise convolutional neural networks, in: Proceedings of the IEEE/CVF Conference on Computer Vision and Pattern Recognition, pp. 984–993.
- Huang, J., You, S., 2016. Point cloud labeling using 3d convolutional neural network, in: 2016 23rd International Conference on Pattern Recognition (ICPR), IEEE. pp. 2670–2675.
- Huang, Q., Wang, W., Neumann, U., 2018. Recurrent slice networks for 3d segmentation of point clouds, in: Proceedings of the IEEE/CVF Conference on Computer Vision and Pattern Recognition, pp. 2626–2635.
- Iandola, F., Han, S., Moskewicz, M., Ashraf, K., Dally, W., Keutzer, K., 2016. Squeezenet: Alexnet-level accuracy with 50x fewer parameters and < 0.5 mb model size. *arXiv preprint arXiv:1602.07360*.
- Ioannidou, A., Chatzilaris, E., Nikolopoulos, S., Kompatsiaris, I., 2017. Deep learning advances in computer vision with 3d data: A survey. *ACM Computing Surveys* 50, 1–38.
- Ivanec, B.J., 2016. Depth estimation by convolutional neural networks. Ph.D. thesis. Master thesis, Brno University of Technology.
- Jampani, V., Kiefel, M., Gehler, P.V., 2016. Learning sparse high dimensional filters: Image filtering, dense crfs and bilateral neural networks, in: Proceedings of the IEEE/CVF Conference on Computer Vision and Pattern Recognition, pp. 4452–4461.
- Jaritz, M., Gu, J., Su, H., 2019. Multi-view pointnet for 3d scene understanding, in: Proceedings of the IEEE/CVF International Conference on Computer Vision Workshops, pp. 0–0.

- Jeong, J., Yoon, T.S., Park, J.B., 2018. Multimodal sensor-based semantic 3d mapping for a large-scale environment. *Expert Systems with Applications* 105, 1–10.
- Jiang, H., Yan, F., Cai, J., Zheng, J., Xiao, J., 2020a. End-to-end 3d point cloud instance segmentation without detection, in: *Proceedings of the IEEE/CVF Conference on Computer Vision and Pattern Recognition*, pp. 12796–12805.
- Jiang, J., Zhang, Z., Huang, Y., Zheng, L., 2017. Incorporating depth into both cnn and crf for indoor semantic segmentation, in: *Processing of the IEEE International Conference on Software Engineering and Service Science, IEEE*. pp. 525–530.
- Jiang, L., Zhao, H., Shi, S., Liu, S., Fu, C., Jia, J., 2020b. Pointgroup: Dual-set point grouping for 3d instance segmentation, in: *Proceedings of the IEEE/CVF Conference on Computer Vision and Pattern Recognition*, pp. 4867–4876.
- Jiang, M., Wu, Y., Zhao, T., Zhao, Z., Lu, C., 2018. Pointsift: A sift-like network module for 3d point cloud semantic segmentation. *arXiv preprint arXiv:1807.00652*.
- Kalogerakis, E., Averkiou, M., Maji, S., Chaudhuri, S., 2017. 3d shape segmentation with projective convolutional networks, in: *Proceedings of the IEEE/CVF Conference on Computer Vision and Pattern Recognition*, pp. 3779–3788.
- Kirillov, A., Mintun, E., Ravi, N., Mao, H., Rolland, C., Gustafson, L., Xiao, T., Whitehead, S., Berg, A.C., Lo, W.Y., et al., 2023. Segment anything. *arXiv preprint arXiv:2304.02643*.
- Klokov, R., Lempitsky, V., 2017. Escape from cells: Deep kd-networks for the recognition of 3d point cloud models, in: *Proceedings of the IEEE/CVF International Conference on Computer Vision*, pp. 863–872.
- Kochanov, D., Ošep, A., Stückler, J., Leibe, B., 2016. Scene flow propagation for semantic mapping and object discovery in dynamic street scenes, in: *Proc. IEEE Int. Conf. Intell. Rob. Syst., IEEE*. pp. 1785–1792.
- Komarichev, A., Zhong, Z., Hua, J., 2019. A-cnn: Annularly convolutional neural networks on point clouds, in: *Proceedings of the IEEE/CVF Conference on Computer Vision and Pattern Recognition*, pp. 7421–7430.
- Kong, L., Liu, Y., Chen, R., Ma, Y., Zhu, X., Li, Y., Hou, Y., Qiao, Y., Liu, Z., 2023. Rethinking range view representation for lidar segmentation. *arXiv preprint arXiv:2303.05367*.
- Lahoud, J., Ghanem, B., Pollefeys, M., Oswald, M., 2019. 3d instance segmentation via multi-task metric learning, in: *Proceedings of the IEEE/CVF International Conference on Computer Vision*, pp. 9256–9266.
- Lai, X., Chen, Y., Lu, F., Liu, J., Jia, J., 2023. Spherical transformer for lidar-based 3d recognition, in: *Proceedings of the IEEE/CVF Conference on Computer Vision and Pattern Recognition*, pp. 17545–17555.
- Lai, X., Liu, J., Jiang, L., Wang, L., Zhao, H., Liu, S., Qi, X., Jia, J., 2022. Stratified transformer for 3d point cloud segmentation, in: *Proceedings of the IEEE/CVF Conference on Computer Vision and Pattern Recognition*, pp. 8500–8509.
- Landrieu, L., Simonovsky, M., 2018. Large-scale point cloud semantic segmentation with superpoint graphs, in: *Proceedings of the IEEE/CVF Conference on Computer Vision and Pattern Recognition*, pp. 4558–4567.
- Lawin, F., Danelljan, M., Tosteberg, P., Bhat, G., Khan, F., Felsberg, M., 2017. Deep projective 3d semantic segmentation, in: *Computer Analysis of Images and Patterns, Springer*. pp. 95–107.
- Le, T., Duan, Y., 2018. Pointgrid: A deep network for 3d shape understanding, in: *Proceedings of the IEEE/CVF Conference on Computer Vision and Pattern Recognition*, pp. 9204–9214.
- Lei, H., Akhtar, N., Mian, A., 2019. Octree guided cnn with spherical kernels for 3d point clouds, in: *Proceedings of the IEEE/CVF Conference on Computer Vision and Pattern Recognition*, pp. 9631–9640.
- Lei, H., Akhtar, N., Mian, A., 2020. Spherical kernel for efficient graph convolution on 3d point clouds. *IEEE Transactions on Pattern Analysis and Machine Intelligence*.
- Lei, H., Akhtar, N., Shah, M., Mian, A., 2023. Mesh convolution with continuous filters for 3-d surface parsing. *IEEE Transactions on Neural Networks and Learning Systems*.
- Li, G., Muller, M., Thabet, A., Ghanem, B., 2019a. Deepgcns: Can gcns go as deep as cnns?, in: *Proceedings of the IEEE/CVF International Conference on Computer Vision*, pp. 9267–9276.
- Li, J., Chen, B.M., Hee Lee, G., 2018a. So-net: Self-organizing network for point cloud analysis, in: *Proceedings of the IEEE/CVF Conference on Computer Vision and Pattern Recognition*, pp. 9397–9406.
- Li, Y., Bu, R., Sun, M., Wu, W., Di, X., Chen, B., 2018b. Pointcnn: Convolution on x-transformed points. *Advances in Neural Information Processing Systems* 31, 820–830.
- Li, Y., Ma, L., Zhong, Z., Cao, D., Li, J., 2019b. Tgnet: Geometric graph cnn on 3-d point cloud segmentation. *IEEE Transactions on Geoscience and Remote Sensing* 58, 3588–3600.
- Li, Z., Gan, Y., Liang, X., Yu, Y., Cheng, H., Lin, L., 2016. Lstmcf: Unifying context modeling and fusion with lstms for rgb-d scene labeling, in: *Proceedings of the European Conference on Computer Vision, Springer*. pp. 541–557.
- Lian, Q., Li, P., Chen, X., 2022. Monojsjg: Joint semantic and geometric cost volume for monocular 3d object detection, in: *Proceedings of the IEEE/CVF Conference on Computer Vision and Pattern Recognition*, pp. 1070–1079.
- Liang, Z., Li, Z., Xu, S., Tan, M., Jia, K., 2021. Instance segmentation in 3d scenes using semantic superpoint tree networks, in: *Proceedings of the IEEE/CVF International Conference on Computer Vision*, pp. 2783–2792.
- Liang, Z., Yang, M., Deng, L., Wang, C., Wang, B., 2019a. Hierarchical depthwise graph convolutional neural network for 3d semantic segmentation of point clouds, in: *Processing of the IEEE International Conference on Robotics and Automation, IEEE*. pp. 8152–8158.
- Liang, Z., Yang, M., Wang, C., 2019b. 3d graph embedding learning with a structure-aware loss function for point cloud semantic instance segmentation. *arXiv preprint arXiv:1902.05247*.
- Lin, D., Chen, G., Cohen-Or, D., Heng, P., Huang, H., 2017. Cascaded feature network for semantic segmentation of rgb-d images, in: *Proceedings of the IEEE/CVF International Conference on Computer Vision*, pp. 1311–1319.
- Liu, C., Furukawa, Y., 2019. Masc: multi-scale affinity with sparse convolution for 3d instance segmentation. *arXiv preprint arXiv:1902.04478*.
- Liu, F., Li, S., Zhang, L., Zhou, C., Ye, R., Wang, Y., Lu, J., 2017. 3dcnn-dqn-rnn: A deep reinforcement learning framework for semantic parsing of large-scale 3d point clouds, in: *Proceedings of the IEEE/CVF International Conference on Computer Vision*, pp. 5678–5687.
- Liu, F., Shen, C., Lin, G., Reid, I., 2015. Learning depth from single monocular images using deep convolutional neural fields. *IEEE Transactions on Pattern Analysis and Machine Intelligence* 38, 2024–2039.
- Liu, H., Wu, W., Wang, X., Qian, Y., 2018a. Rgb-d joint modelling with scene geometric information for indoor semantic segmentation. *Multimed. Tools. Appl.* 77, 22475–22488.
- Liu, J., Wang, Y., Li, Y., Fu, J., Li, J., Lu, H., 2018b. Collaborative deconvolutional neural networks for joint depth estimation and semantic segmentation. *IEEE Trans. Neural Netw. Learn. Syst.* 29, 5655–5666.
- Liu, W., Sun, J., Li, W., Hu, T., Wang, P., 2019a. Deep learning on point clouds and its application: A survey. *Sensors* 19, 4188.
- Liu, Y., Yang, S., Li, B., Zhou, W., Xu, J., Li, H., Lu, Y., 2018c. Affinity derivation and graph merge for instance segmentation, in: *Proceedings of the European Conference on Computer Vision*, pp. 686–703.
- Liu, Z., Tang, H., Lin, Y., Han, S., 2019b. Point-voxel cnn for efficient 3d deep learning, in: *Advances in Neural Information Processing Systems*, pp. 965–975.
- Lowe, D.G., 2004. Distinctive image features from scale-invariant keypoints. *International journal of computer vision* 60, 91–110.
- Ma, L., Stückler, J., Kerl, C., Cremers, D., 2017. Multi-view deep learning for consistent semantic mapping with rgb-d cameras, in: *Proc. IEEE Int. Conf. Intell. Rob. Syst., IEEE*. pp. 598–605.
- Ma, Y., Guo, Y., Liu, H., Lei, Y., Wen, G., 2020. Global context reasoning for semantic segmentation of 3d point clouds, in: *Proceedings of the IEEE/CVF Winter Conference on Applications of Computer Vision*, pp. 2931–2940.

- Maturana, D., Scherer, S., 2015. Voxnet: A 3d convolutional neural network for real-time object recognition, in: Proc. IEEE Int. Conf. Intell. Rob. Syst., IEEE. pp. 922–928.
- McCormac, J., Handa, A., Davison, A., Leutenegger, S., 2017. Semanticfusion: Dense 3d semantic mapping with convolutional neural networks, in: Proceedings of the IEEE International Conference on Robotics and Automation, IEEE. pp. 4628–4635.
- Meng, H., Gao, L., Lai, Y., Manocha, D., 2019. Vv-net: Voxel vae net with group convolutions for point cloud segmentation, in: Proceedings of the IEEE/CVF International Conference on Computer Vision, pp. 8500–8508.
- Meyer, G.P., Charland, J., Hegde, D., Laddha, A., Vallespi-Gonzalez, C., 2019. Sensor fusion for joint 3d object detection and semantic segmentation, in: Proceedings of the IEEE/CVF Conference on Computer Vision and Pattern Recognition Workshops, pp. 0–0.
- Milioto, A., Vizzo, I., Behley, J., Stachniss, C., 2019. Rangenet++: Fast and accurate lidar semantic segmentation, in: Proc. IEEE Int. Conf. Intell. Rob. Syst., IEEE. pp. 4213–4220.
- Morton, G.M., 1966. A computer oriented geodetic data base and a new technique in file sequencing .
- Mousavian, A., Pirsaviash, H., Košecká, J., 2016. Joint semantic segmentation and depth estimation with deep convolutional networks, in: Processing of the International Conference on 3D Vision, IEEE. pp. 611–619.
- Narita, G., Seno, T., Ishikawa, T., Kaji, Y., 2019. Panopticfusion: Online volumetric semantic mapping at the level of stuff and things. arXiv preprint arXiv:1903.01177 .
- Naseer, M., Khan, S., Porikli, F., 2018. Indoor scene understanding in 2.5/3d for autonomous agents: A survey. IEEE Access 7, 1859–1887.
- Ngo, T.D., Hua, B.S., Nguyen, K., 2023. Isbnet: a 3d point cloud instance segmentation network with instance-aware sampling and box-aware dynamic convolution, in: Proceedings of the IEEE/CVF Conference on Computer Vision and Pattern Recognition, pp. 13550–13559.
- Park, C., Jeong, Y., Cho, M., Park, J., 2022. Fast point transformer, in: Proceedings of the IEEE/CVF Conference on Computer Vision and Pattern Recognition, pp. 16949–16958.
- Park, J., Kim, C., Kim, S., Jo, K., 2023. Pscnet: Fast 3d semantic segmentation of lidar point cloud for autonomous car using point convolution and sparse convolution network. Expert Systems with Applications 212, 118815.
- Pham, Q., Hua, B., Nguyen, T., Yeung, S., 2019a. Real-time progressive 3d semantic segmentation for indoor scenes, in: Proceedings of the IEEE/CVF Winter Conference on Applications of Computer Vision, IEEE. pp. 1089–1098.
- Pham, Q.H., Nguyen, T., Hua, B.S., Roig, G., Yeung, S.K., 2019b. Jsis3d: joint semantic-instance segmentation of 3d point clouds with multi-task pointwise networks and multi-value conditional random fields, in: Proceedings of the IEEE/CVF Conference on Computer Vision and Pattern Recognition, pp. 8827–8836.
- Qi, C.R., Su, H., Mo, K., Guibas, L.J., 2017a. Pointnet: Deep learning on point sets for 3d classification and segmentation, in: Proceedings of the IEEE/CVF Conference on Computer Vision and Pattern Recognition, pp. 652–660.
- Qi, C.R., Yi, L., Su, H., Guibas, L.J., 2017b. Pointnet++: Deep hierarchical feature learning on point sets in a metric space. Advances in Neural Information Processing Systems 30, 5099–5108.
- Qi, X., Liao, R., Jia, J., Fidler, S., Urtasun, R., 2017c. 3d graph neural networks for rgb-d semantic segmentation, in: Proceedings of the IEEE/CVF International Conference on Computer Vision, pp. 5199–5208.
- Qian, G., Li, Y., Peng, H., Mai, J., Hammoud, H.A.A.K., Elhoseiny, M., Ghanem, B., 2022. Pointnext: Revisiting pointnet++ with improved training and scaling strategies. arXiv preprint arXiv:2206.04670 .
- Raj, A., Maturana, D., Scherer, S., 2015. Multi-scale convolutional architecture for semantic segmentation. Robotics Institute, Carnegie Mellon University, Tech. Rep. CMU-RITR-15-21 .
- Ran, H., Liu, J., Wang, C., 2022. Surface representation for point clouds, in: Proceedings of the IEEE/CVF Conference on Computer Vision and Pattern Recognition, pp. 18942–18952.
- Rethage, D., Wald, J., Sturm, J., Navab, N., Tombari, F., 2018. Fully-convolutional point networks for large-scale point clouds, in: Proceedings of the European Conference on Computer Vision, pp. 596–611.
- Riegler, G., Osman Ulusoy, A., Geiger, A., 2017. Octnet: Learning deep 3d representations at high resolutions, in: Proceedings of the IEEE/CVF Conference on Computer Vision and Pattern Recognition, pp. 3577–3586.
- Riemenschneider, H., Bódis-Szomorú, A., Weissenberg, J., Van Gool, L., 2014. Learning where to classify in multi-view semantic segmentation, in: Proceedings of the European Conference on Computer Vision, Springer. pp. 516–532.
- Rosu, R.A., Schütt, P., Quenzel, J., Behnke, S., 2019. Latticenet: Fast point cloud segmentation using permutohedral lattices. arXiv preprint arXiv:1912.05905 .
- Roynard, X., Deschaud, J., Goulette, F., 2018. Paris-lille-3d: A large and high-quality ground-truth urban point cloud dataset for automatic segmentation and classification. The International Journal of Robotics Research 37, 545–557.
- Shen, Y., Feng, C., Yang, Y., Tian, D., 2018. Mining point cloud local structures by kernel correlation and graph pooling, in: Proceedings of the IEEE/CVF Conference on Computer Vision and Pattern Recognition, pp. 4548–4557.
- Shi, H., Lin, G., Wang, H., Hung, T.Y., Wang, Z., 2020. Spsequencenet: Semantic segmentation network on 4d point clouds, in: Proceedings of the IEEE/CVF Conference on Computer Vision and Pattern Recognition, pp. 4574–4583.
- Shi, H., Wei, J., Li, R., Liu, F., Lin, G., 2022. Weakly supervised segmentation on outdoor 4d point clouds with temporal matching and spatial graph propagation, in: Proceedings of the IEEE/CVF Conference on Computer Vision and Pattern Recognition, pp. 11840–11849.
- Silberman, N., Fergus, R., 2011. Indoor scene segmentation using a structured light sensor, in: Proceedings of the IEEE/CVF International Conference on Computer Vision Worksh., IEEE. pp. 601–608.
- Silberman, N., Hoiem, D., Kohli, P., Fergus, R., 2012. Indoor segmentation and support inference from rgb-d images, in: Proceedings of the European Conference on Computer Vision, Springer. pp. 746–760.
- Simonovsky, M., Komodakis, N., 2017. Dynamic edge-conditioned filters in convolutional neural networks on graphs, in: Proceedings of the IEEE/CVF Conference on Computer Vision and Pattern Recognition, pp. 3693–3702.
- Song, S., Lichtenberg, S.P., Xiao, J., 2015. Sun rgb-d: A rgb-d scene understanding benchmark suite, in: Proceedings of the IEEE/CVF Conference on Computer Vision and Pattern Recognition, pp. 567–576.
- Song, Y., Chen, X., Li, J., Zhao, Q., 2017. Embedding 3d geometric features for rigid object part segmentation, in: Proceedings of the IEEE/CVF International Conference on Computer Vision, pp. 580–588.
- Su, H., Jampani, V., Sun, D., Maji, S., Kalogerakis, E., Yang, M.H., Kautz, J., 2018. Splatnet: Sparse lattice networks for point cloud processing, in: Proceedings of the IEEE/CVF Conference on Computer Vision and Pattern Recognition, pp. 2530–2539.
- Su, H., Maji, S., Kalogerakis, E., Learned-Miller, E., 2015. Multi-view convolutional neural networks for 3d shape recognition, in: Proceedings of the IEEE/CVF International Conference on Computer Vision, pp. 945–953.
- Su, Y., Xu, X., Jia, K., 2023. Weakly supervised 3d point cloud segmentation via multi-prototype learning. IEEE Transactions on Circuits and Systems for Video Technology .
- Tatarchenko, M., Park, J., Koltun, V., Zhou, Q.Y., 2018. Tangent convolutions for dense prediction in 3d, in: Proceedings of the IEEE/CVF Conference on Computer Vision and Pattern Recognition, pp. 3887–3896.
- Tchapmi, L., Choy, C., Armeni, I., Gwak, J., Savarese, S., 2017. Segcloud: Semantic segmentation of 3d point clouds, in: Processing of the International Conference on 3D Vision, IEEE. pp. 537–547.
- Thomas, H., Qi, C.R., Deschaud, J.E., Marcotegui, B., Goulette, F., Guibas, L.J., 2019. Kpconv: Flexible and deformable convolution for point clouds, in: Proceedings of the IEEE/CVF International Conference on Computer Vision, pp. 6411–6420.

- Valipour, S., Siam, M., Jagersand, M., Ray, N., 2017. Recurrent fully convolutional networks for video segmentation, in: Proceedings of the IEEE/CVF Winter Conference on Applications of Computer Vision, IEEE. pp. 29–36.
- Verma, N., Boyer, E., Verbeek, J., 2018. Feastnet: Feature-steered graph convolutions for 3d shape analysis, in: Proceedings of the IEEE/CVF Conference on Computer Vision and Pattern Recognition, pp. 2598–2606.
- Vu, T., Kim, K., Luu, T.M., Nguyen, T., Yoo, C.D., 2022. Softgroup for 3d instance segmentation on point clouds, in: Proceedings of the IEEE/CVF Conference on Computer Vision and Pattern Recognition, pp. 2708–2717.
- Wang, C., Samari, B., Siddiqi, K., 2018a. Local spectral graph convolution for point set feature learning, in: Proceedings of the European Conference on Computer Vision, pp. 52–66.
- Wang, J., Li, X., Sullivan, A., Abbott, L., Chen, S., 2022. Pointmotionnet: Point-wise motion learning for large-scale lidar point clouds sequences, in: Proceedings of the IEEE/CVF Conference on Computer Vision and Pattern Recognition, pp. 4419–4428.
- Wang, J., Wang, Z., Tao, D., See, S., Wang, G., 2016. Learning common and specific features for rgb-d semantic segmentation with deconvolutional networks, in: Proceedings of the European Conference on Computer Vision, Springer. pp. 664–679.
- Wang, P., Gan, Y., Shui, P., Yu, F., Zhang, Y., Chen, S., Sun, Z., 2018b. 3d shape segmentation via shape fully convolutional networks. *Computers & Graphics* 70, 128–139.
- Wang, P., Shen, X., Lin, Z., Cohen, S., Price, B., Yuille, A., 2015. Towards unified depth and semantic prediction from a single image, in: Proceedings of the IEEE/CVF Conference on Computer Vision and Pattern Recognition, pp. 2800–2809.
- Wang, P.S., Liu, Y., Guo, Y.X., Sun, C.Y., Tong, X., 2017. O-cnn: Octree-based convolutional neural networks for 3d shape analysis. *ACM Transactions on Graphics* 36, 1–11.
- Wang, S., Suo, S., Ma, W.C., Pokrovsky, A., Urtasun, R., 2018c. Deep parametric continuous convolutional neural networks, in: Proceedings of the IEEE/CVF Conference on Computer Vision and Pattern Recognition, pp. 2589–2597.
- Wang, W., Neumann, U., 2018. Depth-aware cnn for rgb-d segmentation, in: Proceedings of the European Conference on Computer Vision, pp. 135–150.
- Wang, W., Yu, R., Huang, Q., Neumann, U., 2018d. Sgpn: Similarity group proposal network for 3d point cloud instance segmentation, in: Proceedings of the IEEE/CVF Conference on Computer Vision and Pattern Recognition, pp. 2569–2578.
- Wang, X., Liu, S., Shen, X., Shen, C., Jia, J., 2019a. Associatively segmenting instances and semantics in point clouds, in: Proceedings of the IEEE/CVF Conference on Computer Vision and Pattern Recognition, pp. 4096–4105.
- Wang, Y., Asafi, S., Van Kaick, O., Zhang, H., Cohen-Or, D., Chen, B., 2012. Active co-analysis of a set of shapes. *ACM Transactions on Graphics* 31, 1–10.
- Wang, Y., Shi, T., Yun, P., Tai, L., Liu, M., 2018e. Pointseg: Real-time semantic segmentation based on 3d lidar point cloud. *arXiv preprint arXiv:1807.06288*.
- Wang, Y., Sun, Y., Liu, Z., Sarma, S.E., Bronstein, M.M., Solomon, J.M., 2019b. Dynamic graph cnn for learning on point clouds. *ACM Transactions on Graphics* 38, 1–12.
- Wang, Z., Lu, F., 2019. Voxsegnet: Volumetric cnns for semantic part segmentation of 3d shapes. *IEEE Transactions on Visualization and Computer Graphics*.
- Wei, L.Y., 2008. Parallel poisson disk sampling. *ACM Transactions on Graphics* 27, 1–9.
- Wei, Y., Liu, H., Xie, T., Ke, Q., Guo, Y., 2022. Spatial-temporal transformer for 3d point cloud sequences, in: Proceedings of the IEEE/CVF Winter Conference on Applications of Computer Vision, pp. 1171–1180.
- Wu, B., Wan, A., Yue, X., Keutzer, K., 2018a. Squeezeseg: Convolutional neural nets with recurrent crf for real-time road-object segmentation from 3d lidar point cloud, in: Proceedings of the IEEE International Conference on Robotics and Automation, IEEE. pp. 1887–1893.
- Wu, B., Zhou, X., Zhao, S., Yue, X., Keutzer, K., 2019a. Squeezesegv2: Improved model structure and unsupervised domain adaptation for road-object segmentation from a lidar point cloud, in: Proceedings of the IEEE International Conference on Robotics and Automation, IEEE. pp. 4376–4382.
- Wu, W., Qi, Z., Fuxin, L., 2019b. Pointconv: Deep convolutional networks on 3d point clouds, in: Proceedings of the IEEE/CVF Conference on Computer Vision and Pattern Recognition, pp. 9621–9630.
- Wu, X., Lao, Y., Jiang, L., Liu, X., Zhao, H., 2022a. Point transformer v2: Grouped vector attention and partition-based pooling. *Advances in Neural Information Processing Systems* 35, 33330–33342.
- Wu, Y., Shi, M., Du, S., Lu, H., Cao, Z., Zhong, W., 2022b. 3d instances as 1d kernels, in: Proceedings of the European Conference on Computer Vision, Springer. pp. 235–252.
- Wu, Y., Wu, Y., Gkioxari, G., Tian, Y., 2018b. Building generalizable agents with a realistic and rich 3d environment. *arXiv preprint arXiv:1801.02209*.
- Wu, Z., Song, S., Khosla, A., Yu, F., Zhang, L., Tang, X., Xiao, J., 2015. 3d shapenets: A deep representation for volumetric shapes, in: Proceedings of the IEEE/CVF Conference on Computer Vision and Pattern Recognition, pp. 1912–1920.
- Wu, Z., Zhou, Z., Allibert, G., Stolz, C., Démonceaux, C., Ma, C., 2022c. Transformer fusion for indoor rgb-d semantic segmentation. Available at SSRN 4251286.
- Xia, Z., Liu, Y., Li, X., Zhu, X., Ma, Y., Li, Y., Hou, Y., Qiao, Y., 2023. Scpnet: Semantic scene completion on point cloud, in: Proceedings of the IEEE/CVF Conference on Computer Vision and Pattern Recognition, pp. 17642–17651.
- Xiang, Y., Fox, D., 2017. Da-rnn: Semantic mapping with data associated recurrent neural networks. *arXiv preprint arXiv:1703.03098*.
- Xiao, A., Huang, J., Guan, D., Zhang, X., Lu, S., Shao, L., 2023. Unsupervised point cloud representation learning with deep neural networks: A survey. *IEEE Transactions on Pattern Analysis and Machine Intelligence*.
- Xie, Y., Jiaoqiao, T., Zhu, X., 2020a. Linking points with labels in 3d: A review of point cloud semantic segmentation. *IEEE Geoscience and Remote Sensing Magazine*.
- Xie, Z., Chen, J., Peng, B., 2020b. Point clouds learning with attention-based graph convolution networks. *Neurocomputing*.
- Xu, C., Wu, B., Wang, Z., Zhan, W., Vajda, P., Keutzer, K., Tomizuka, M., 2020. Squeezesegv3: Spatially-adaptive convolution for efficient point-cloud segmentation. *arXiv preprint arXiv:2004.01803*.
- Xu, H., Dong, M., Zhong, Z., 2017. Directionally convolutional networks for 3d shape segmentation, in: Proceedings of the IEEE/CVF International Conference on Computer Vision, pp. 2698–2707.
- Xu, M., Ding, R., Zhao, H., Qi, X., 2021. Paconv: Position adaptive convolution with dynamic kernel assembling on point clouds, in: Proceedings of the IEEE/CVF Conference on Computer Vision and Pattern Recognition, pp. 3173–3182.
- Xu, Y., Fan, T., Xu, M., Zeng, L., Qiao, Y., 2018. Spidercnn: Deep learning on point sets with parameterized convolutional filters, in: Proceedings of the European Conference on Computer Vision, pp. 87–102.
- Yan, X., Zheng, C., Li, Z., Wang, S., Cui, S., 2020. Pointasnl: Robust point clouds processing using nonlocal neural networks with adaptive sampling, in: Proceedings of the IEEE/CVF conference on computer vision and pattern recognition, pp. 5589–5598.
- Yang, B., Wang, J., Clark, R., Hu, Q., Wang, S., Markham, A., Trigoni, N., 2019. Learning object bounding boxes for 3d instance segmentation on point clouds. *Advances in Neural Information Processing Systems* 32, 6740–6749.
- Yang, S., Huang, Y., Scherer, S., 2017. Semantic 3d occupancy mapping through efficient high order crfs, in: Proc. IEEE Int. Conf. Intell. Rob. Syst., IEEE. pp. 590–597.
- Yang, Y., Xu, Y., Zhang, C., Xu, Z., Huang, J., 2022. Hierarchical vision transformer with channel attention for rgb-d image segmentation, in: Proceedings of the 4th International Symposium on Signal Processing Systems, pp. 68–73.

Ye, X., Li, J., Huang, H., Du, L., Zhang, X., 2018. 3d recurrent neural networks with context fusion for point cloud semantic segmentation, in: Proceedings of the European Conference on Computer Vision, pp. 403–417.

Yi, L., Kim, V., Ceylan, D., Shen, I., Yan, M., Su, H., Lu, C., Huang, Q., Sheffer, A., Guibas, L., 2016. A scalable active framework for region annotation in 3d shape collections. *ACM Transactions on Graphics* 35, 1–12.

Yi, L., Su, H., Guo, X., Guibas, L.J., 2017. Syncspecnn: Synchronized spectral cnn for 3d shape segmentation, in: Proceedings of the IEEE/CVF Conference on Computer Vision and Pattern Recognition, pp. 2282–2290.

Yi, L., Zhao, W., Wang, H., Sung, M., Guibas, L.J., 2019. Gspn: Generative shape proposal network for 3d instance segmentation in point cloud, in: Proceedings of the IEEE/CVF Conference on Computer Vision and Pattern Recognition, pp. 3947–3956.

Ying, X., Chuah, M.C., 2022. Uctnet: Uncertainty-aware cross-modal transformer network for indoor rgb-d semantic segmentation, in: Proceedings of the European Conference on Computer Vision, Springer. pp. 20–37.

Yu, F., Liu, K., Zhang, Y., Zhu, C., Xu, K., 2019. Partnet: A recursive part decomposition network for fine-grained and hierarchical shape segmentation, in: Proceedings of the IEEE/CVF Conference on Computer Vision and Pattern Recognition, pp. 9491–9500.

Yuan, X., Shi, J., Gu, L., 2021. A review of deep learning methods for semantic segmentation of remote sensing imagery. *Expert Systems with Applications* 169, 114417.

Yue, C., Wang, Y., Tang, X., Chen, Q., 2022. Drgcnn: Dynamic region graph convolutional neural network for point clouds. *Expert Systems with Applications* 205, 117663.

Zeng, W., Gevers, T., 2018. 3dcontextnet: Kd tree guided hierarchical learning of point clouds using local and global contextual cues, in: Proceedings of the European Conference on Computer Vision, pp. 0–0.

Zhang, C., Wan, H., Shen, X., Wu, Z., 2022. Patchformer: An efficient point transformer with patch attention, in: Proceedings of the IEEE/CVF Conference on Computer Vision and Pattern Recognition, pp. 11799–11808.

Zhang, Y., Zhou, Z., David, P., Yue, X., Xi, Z., Gong, B., Foroosh, H., 2020. Polarnet: An improved grid representation for online lidar point clouds semantic segmentation, in: Proceedings of the IEEE/CVF Conference on Computer Vision and Pattern Recognition, pp. 9601–9610.

Zhang, Z., Han, X., Dong, B., Li, T., Yin, B., Yang, X., 2023. Point cloud scene completion with joint color and semantic estimation from single rgb-d image. *IEEE Transactions on Pattern Analysis and Machine Intelligence*.

Zhao, C., Sun, L., Purkait, P., Duckett, T., Stolkin, R., 2018. Dense rgb-d semantic mapping with pixel-voxel neural network. *Sensors* 18, 3099.

Zhao, H., Jiang, L., Fu, C.W., Jia, J., 2019a. Pointweb: Enhancing local neighborhood features for point cloud processing, in: Proceedings of the IEEE/CVF Conference on Computer Vision and Pattern Recognition, pp. 5565–5573.

Zhao, H., Jiang, L., Jia, J., Torr, P.H., Koltun, V., 2021. Point transformer, in: Proceedings of the IEEE/CVF International Conference on Computer Vision, pp. 16259–16268.

Zhao, Y., Birdal, T., Deng, H., Tombari, F., 2019b. 3d point capsule networks, in: Proceedings of the IEEE/CVF Conference on Computer Vision and Pattern Recognition, pp. 1009–1018.



Yong He received the M.S. degree from China University of Mining and Technology, Xuzhou, Jiangsu, China, in 2018. He is currently pursuing the Ph.D. degree with Hunan University, Changsha, China, and he is also currently a Visiting Scholar with University of Western Australia, Perth, Australia. His research interests include computer vision, point clouds analysis, and deep learning.



Hongshan Yu received the B.S., M.S. and Ph.D. degrees of Control Science and Technology from electrical and information engineering of Hunan University, Changsha, China, in 2001, 2004 and 2007 respectively. From 2011 to 2012, he worked as a postdoctoral researcher in Laboratory for Computational Neuroscience of University of Pittsburgh, USA. He is currently a professor of Hunan University and associate dean of National Engineering Laboratory for Robot Visual Perception and Control. His research interests include autonomous mobile robot and machine vision.



Xiaoyan Liu received her Ph.D. degree of Process and System Engineering in 2005 from Otto-von-Guericke University Magdeburg, Germany. She is currently a professor of Hunan University. Her research interests include machine vision and pattern recognition.



Zhengeng Yang received the B.S. and M.S. degrees from Central South University, Changsha, China, in 2009 and 2012, respectively. He received the Ph.D. degree from Hunan University, Changsha, China, in 2020. He is currently a post-doctor researcher at Hunan University, Changsha. He was a Visiting Scholar with the University of Pittsburgh, Pittsburgh, PA during 2018 -2020. His research interests include computer vision, image analysis, and machine learning.



Wei Sun received the M.S. and Ph.D. degrees of Control Science and Technology from the Hunan University, Changsha, China, in 1999 and 2002, respectively. He is currently a Professor at Hunan University. His research interests include artificial intelligence, robot control, complex mechanical and electrical control systems, and automotive electronics.



Ajmal Mian is a Professor of computer science with The University of Western Australia. His research interests include 3D computer vision, machine learning, point cloud analysis, human action recognition, and video description. He is Fellow of the International Association for Pattern Recognition and has received several awards including the HBF Mid-Career Scientist of the Year Award, the West Australian Early Career Scientist of the Year Award, the Aspire Professional Development Award, the Vice-Chancellors Mid-Career Research Award, the Outstanding Young Investigator Award, the IAPR Best Scientific Paper Award, the EH Thompson Award, and excellence in Research Supervision Award. He has received three prestigious fellowships and several major research grants from the Australian Research Council, the National Health and Medical Research Council of Australia and the US Dept of Defense DARPA with a total funding of over \$40 Million. He serves as a Senior Editor for the *IEEE Transactions on Neural Networks and Learning Systems*, and Associate Editor for the *IEEE Transactions on Image Processing*, and the *Pattern Recognition Journal*.